Supporting Information for

A Bicyclo[4.2.0]octene-Derived Monomer Provides Completely Linear Alternating Copolymers via Alternating Ring-Opening Metathesis Polymerization (AROMP)

Li Tan, Kathlyn A. Parker, and Nicole S. Sampson**

Department of Chemistry, Stony Brook University, Stony Brook, New York 11794-3400, United States

Table of Contents

Table S1. Molecular weight and $Đ_M$ determined by GPC using polystyrene standards.

Polymer	Temp	Cald. M_n	M_n	M_w	$Đ_M$
poly(4-*alt*-6)$_{16}$	25 °C	5064	10005	22682	2.0
poly(4-*alt*-6)$_{16}$	35 °C	5064	10005	18855	1.8
poly(4-*alt*-6-d$_{10}$)$_{15}$	35 °C	5064	12716	21298	1.7
poly(4-*alt*-6)$_{34}$	35 °C	12504	14552	26512	1.8
poly(4-*alt*-6)$_{36}$	60 °C	12504	11420	24936	2.1
poly(3-*alt*-6-d$_{10}$)$_{6}$	25 °C	1556	2046	7677	3.75

GPC determined M_n is larger than calculated M_n due to the Benoit effect.[1]

Scheme S1. $t_{1/2}$ for each AROM-2 reaction step.

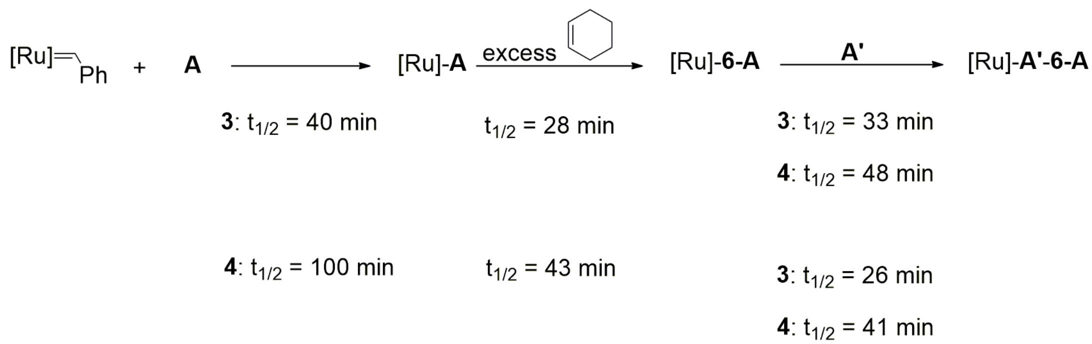

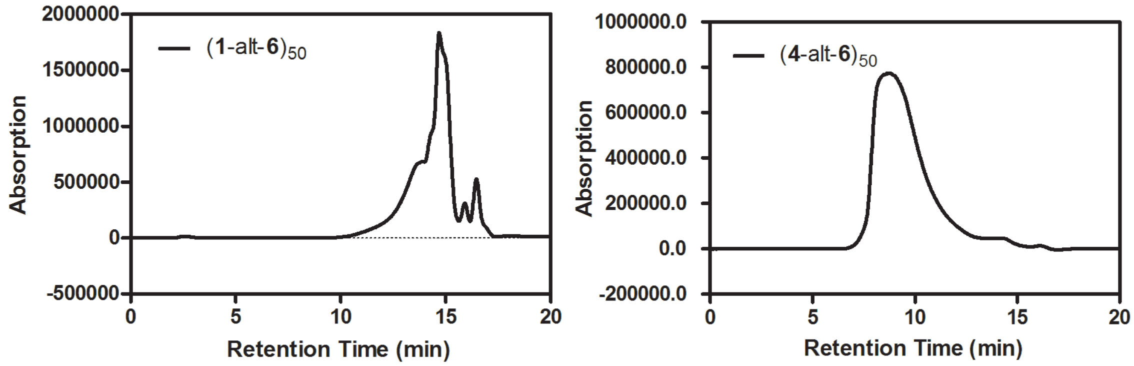

Figure S1. GPC traces of alternating copolymer poly(**4**-*alt*-**6**)$_{50}$ and the corresponding traces of poly(**1**-*alt*-**6**)$_{50}$.

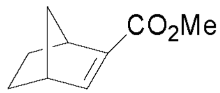

Compound 2

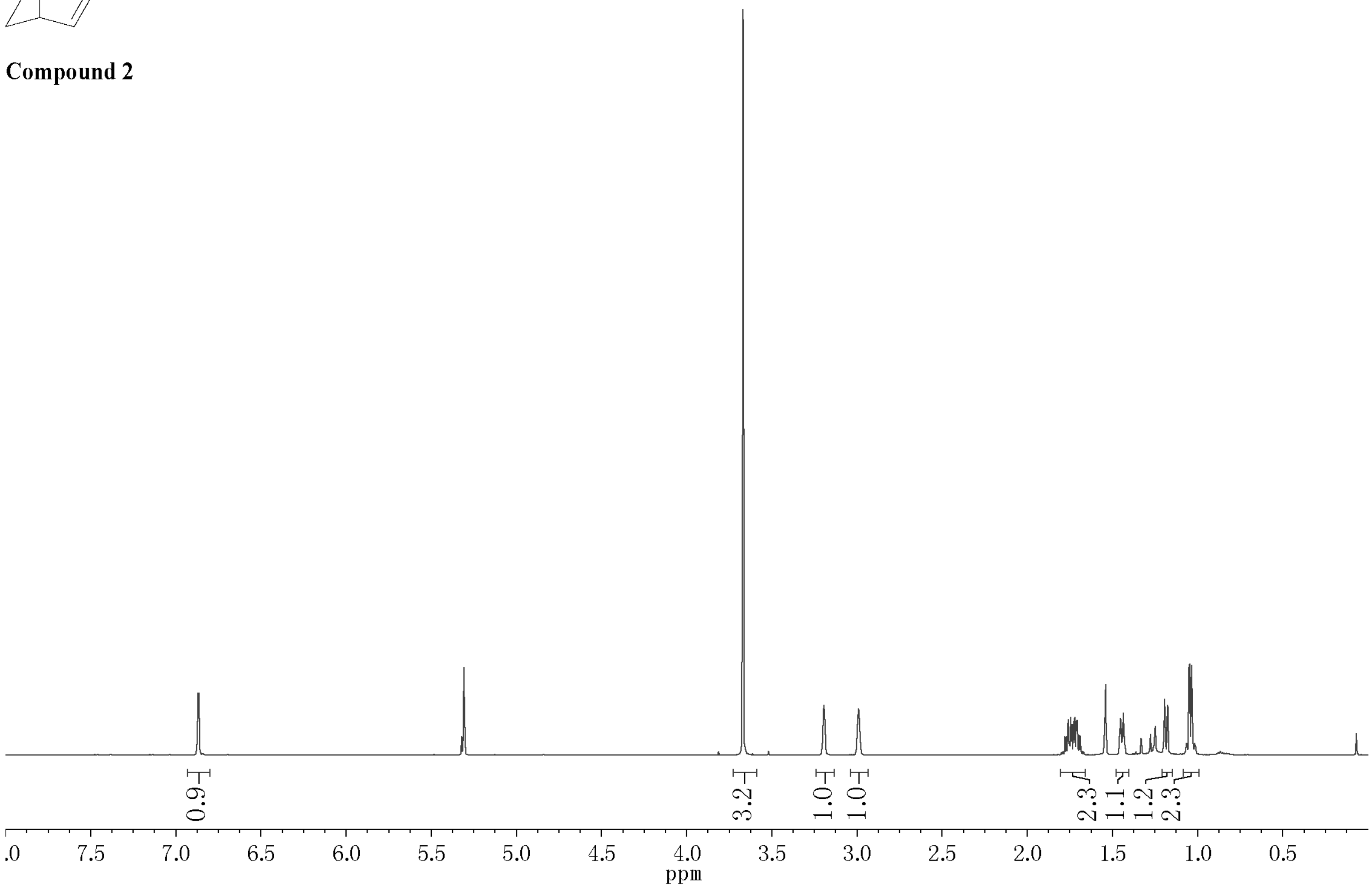

Figure S2. ^{1}H NMR spectrum of **2** in CD_2Cl_2.

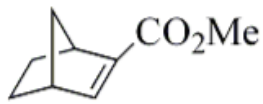

Compound 2

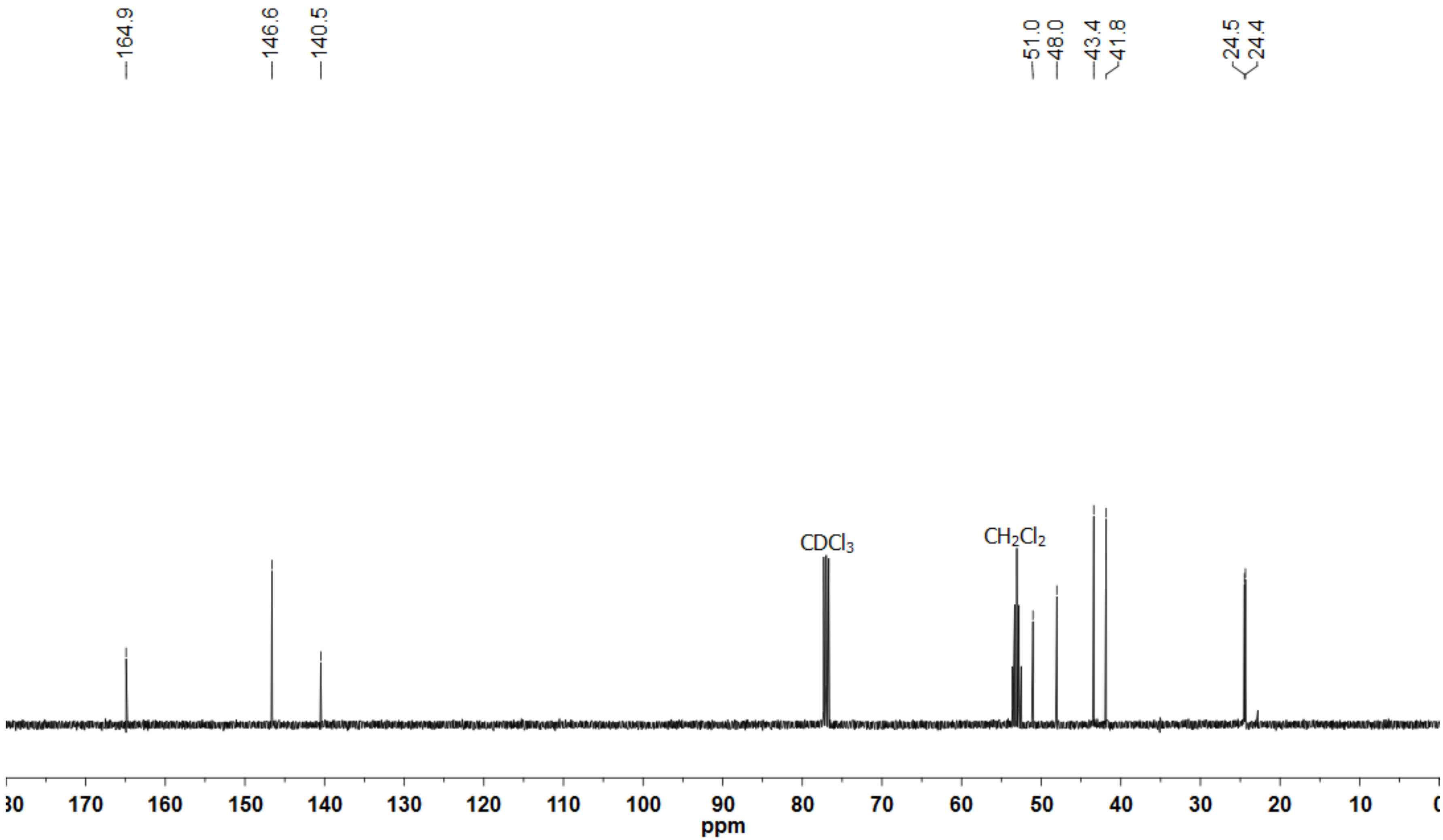

Figure S3. ^{13}C NMR spectrum of **2** in $CDCl_3$.

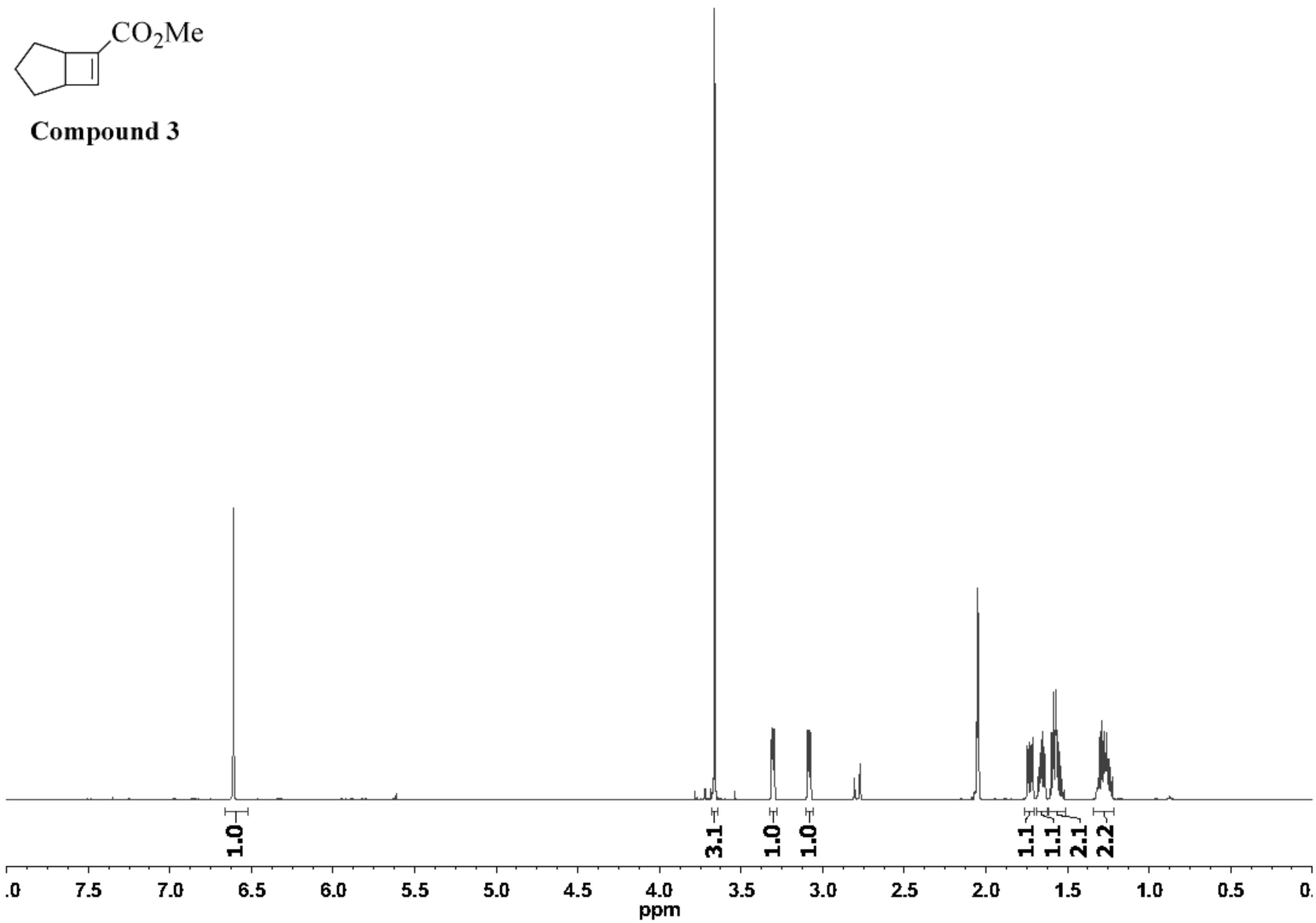

Figure S4. ^{1}H NMR spectrum of **3** in acetone-d_6.

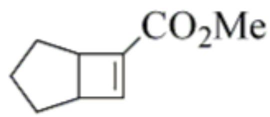

Compound 3

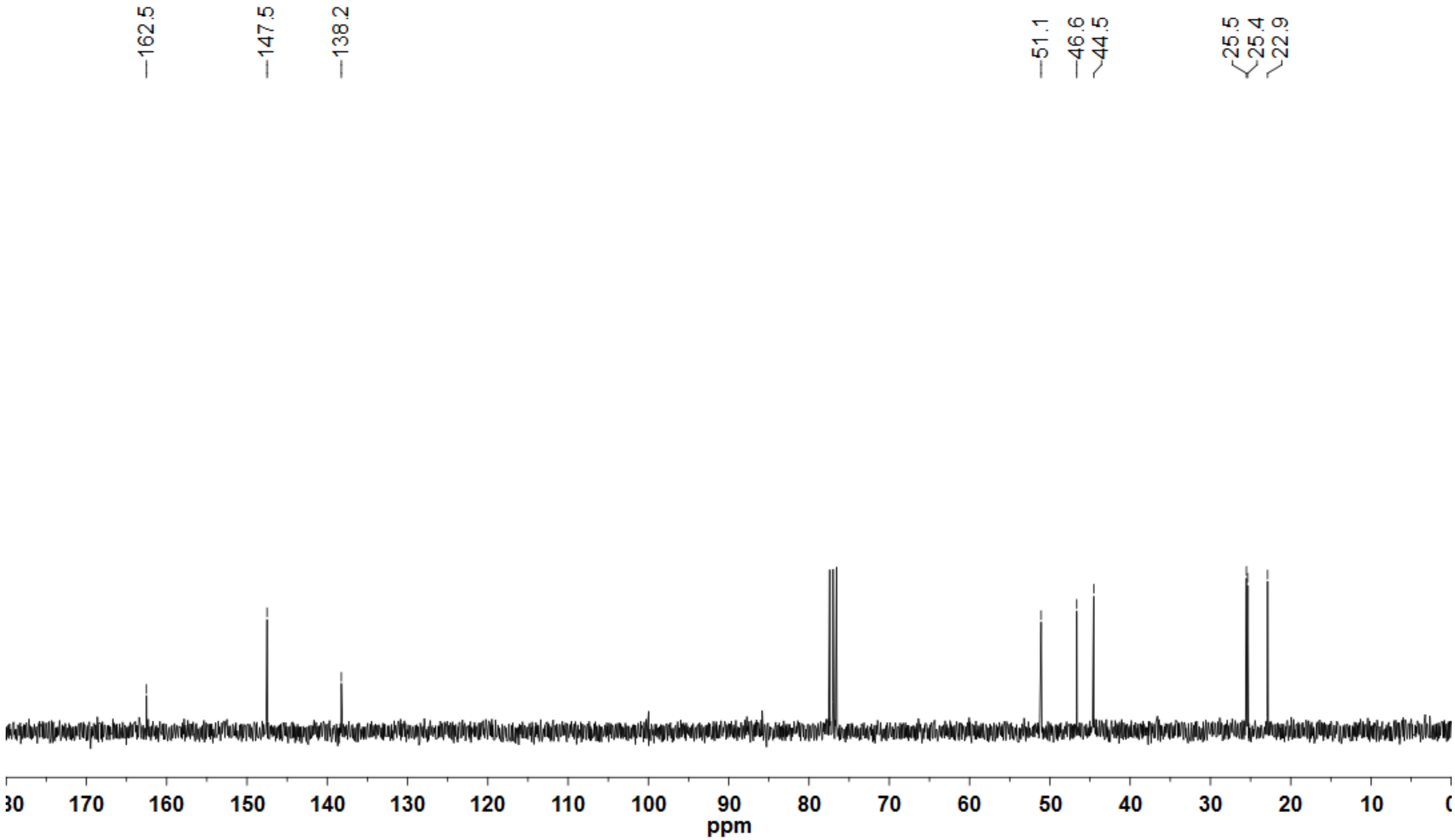

Figure S5. ^{13}C NMR spectrum of **3** in $CDCl_3$.

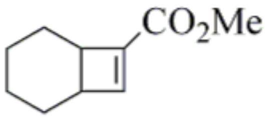

Compound 4

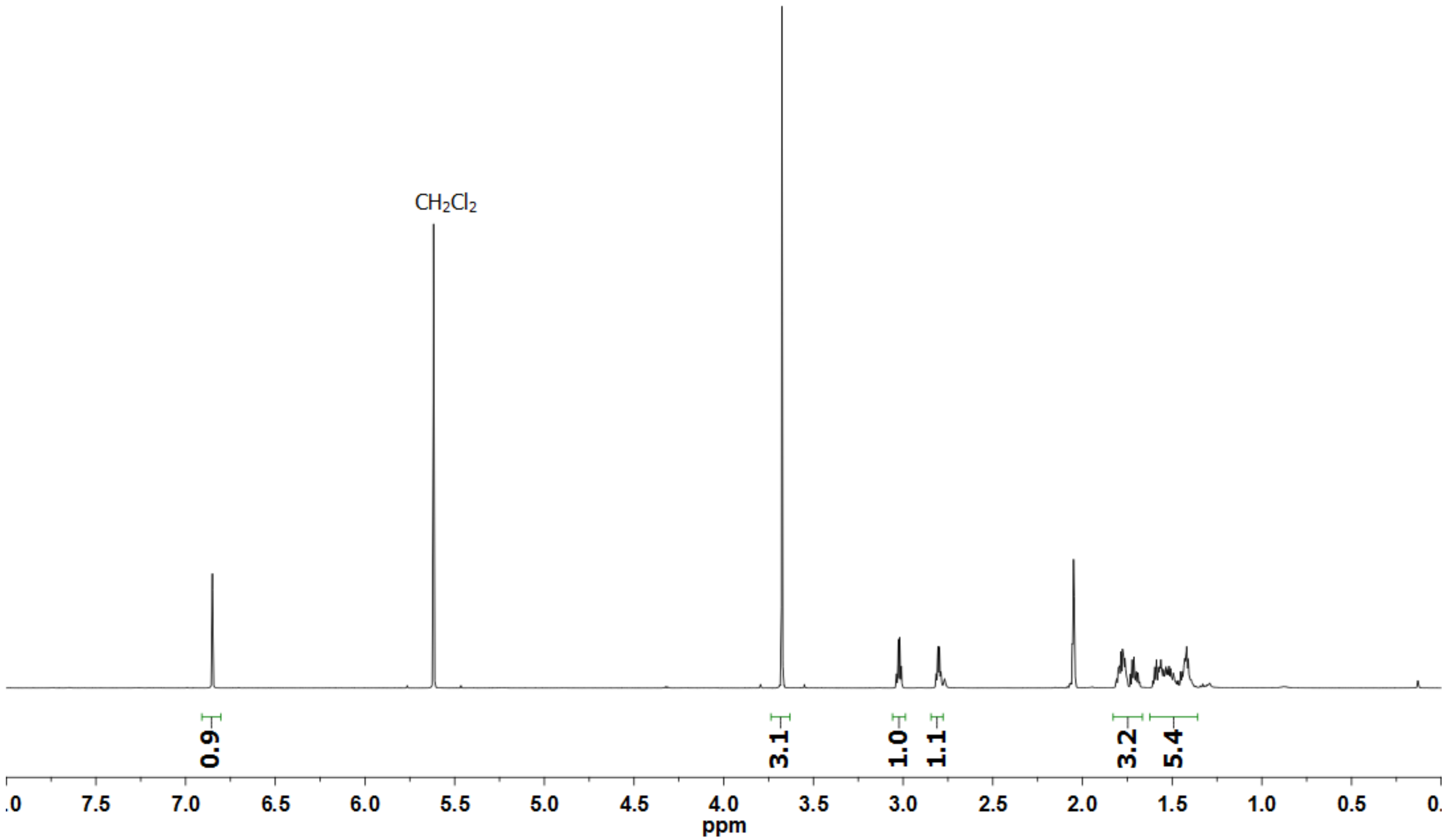

Figure S6. ^{1}H NMR spectrum of **4** in acetone-d_6.

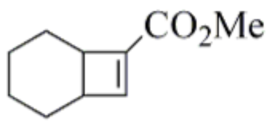

Compound 4

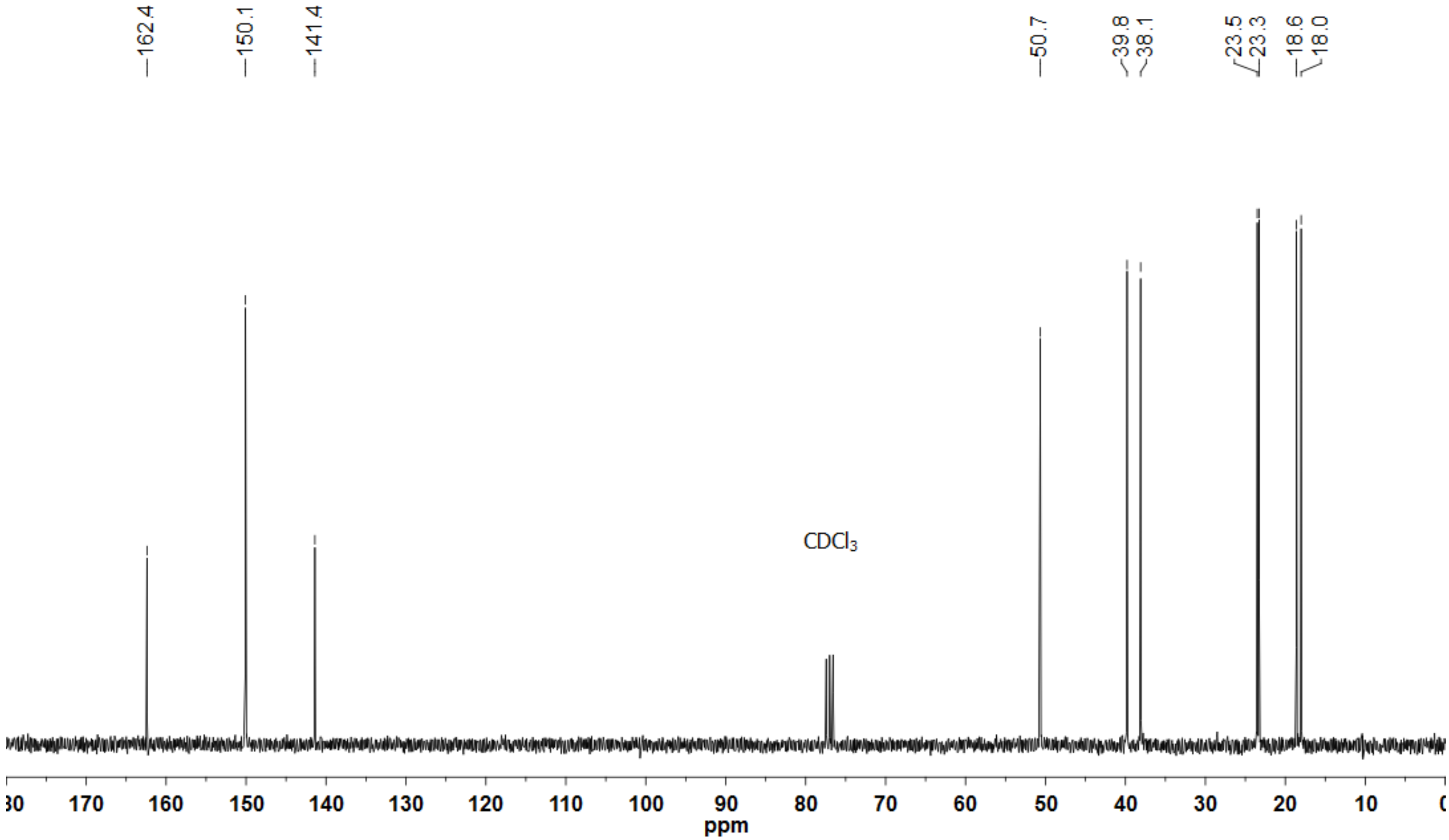

Figure S7. [13]C NMR spectrum of **4** in $CDCl_3$.

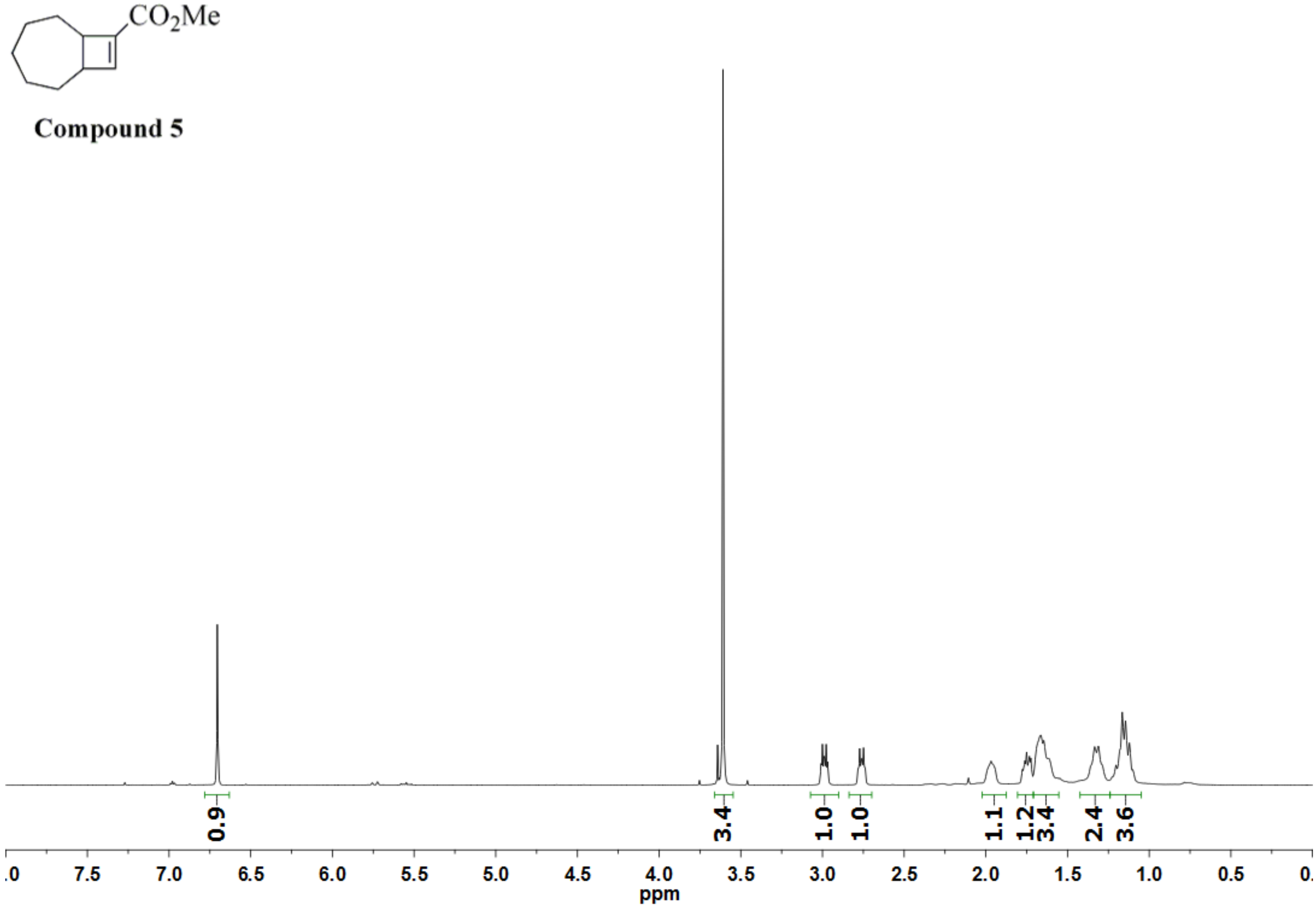

Figure S8. ^{1}H NMR spectrum of **5** in $CDCl_3$.

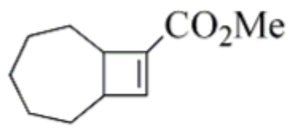

Compound 5

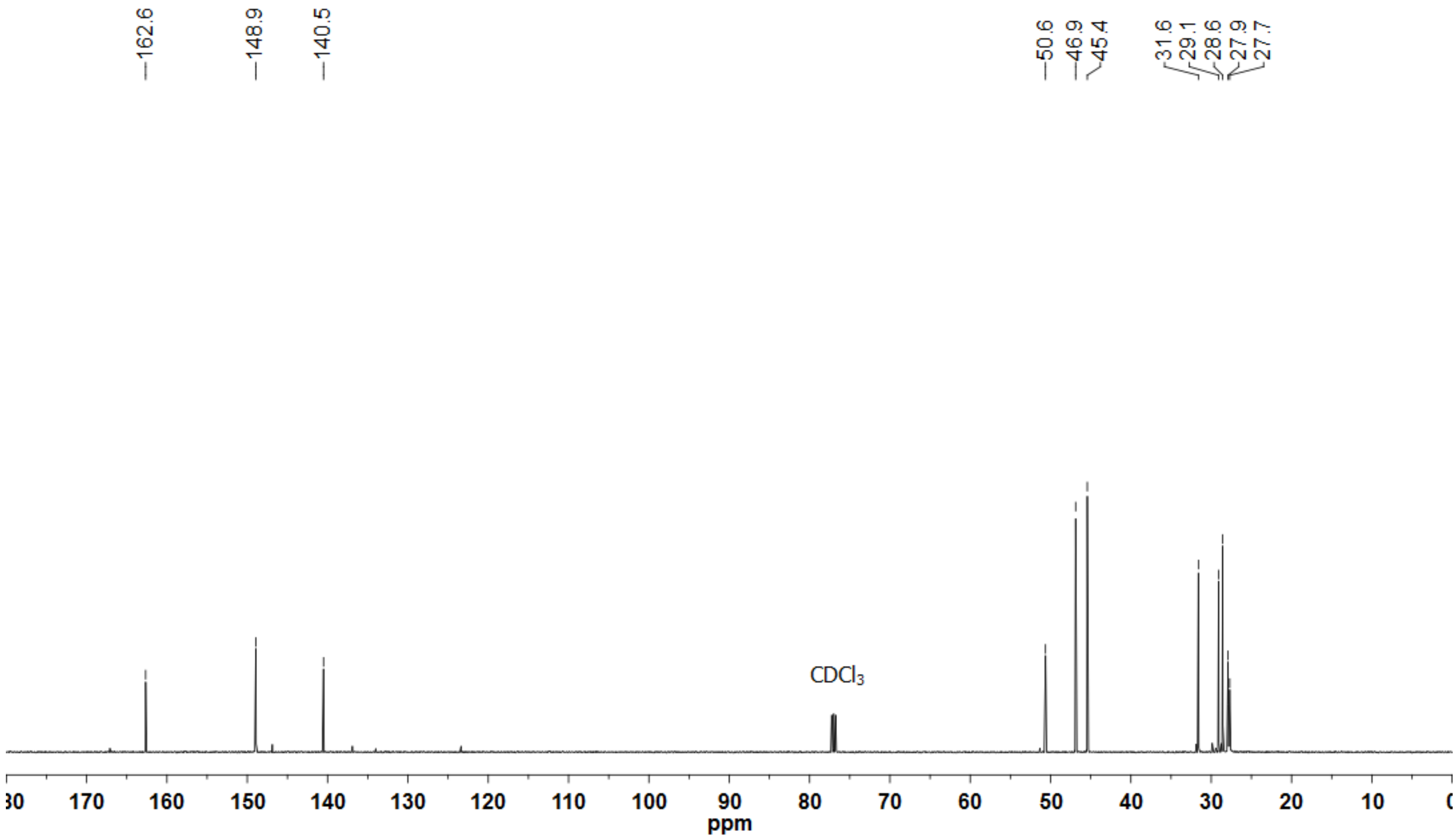

Figure S9. ^{13}C NMR spectrum of **5** in $CDCl_3$.

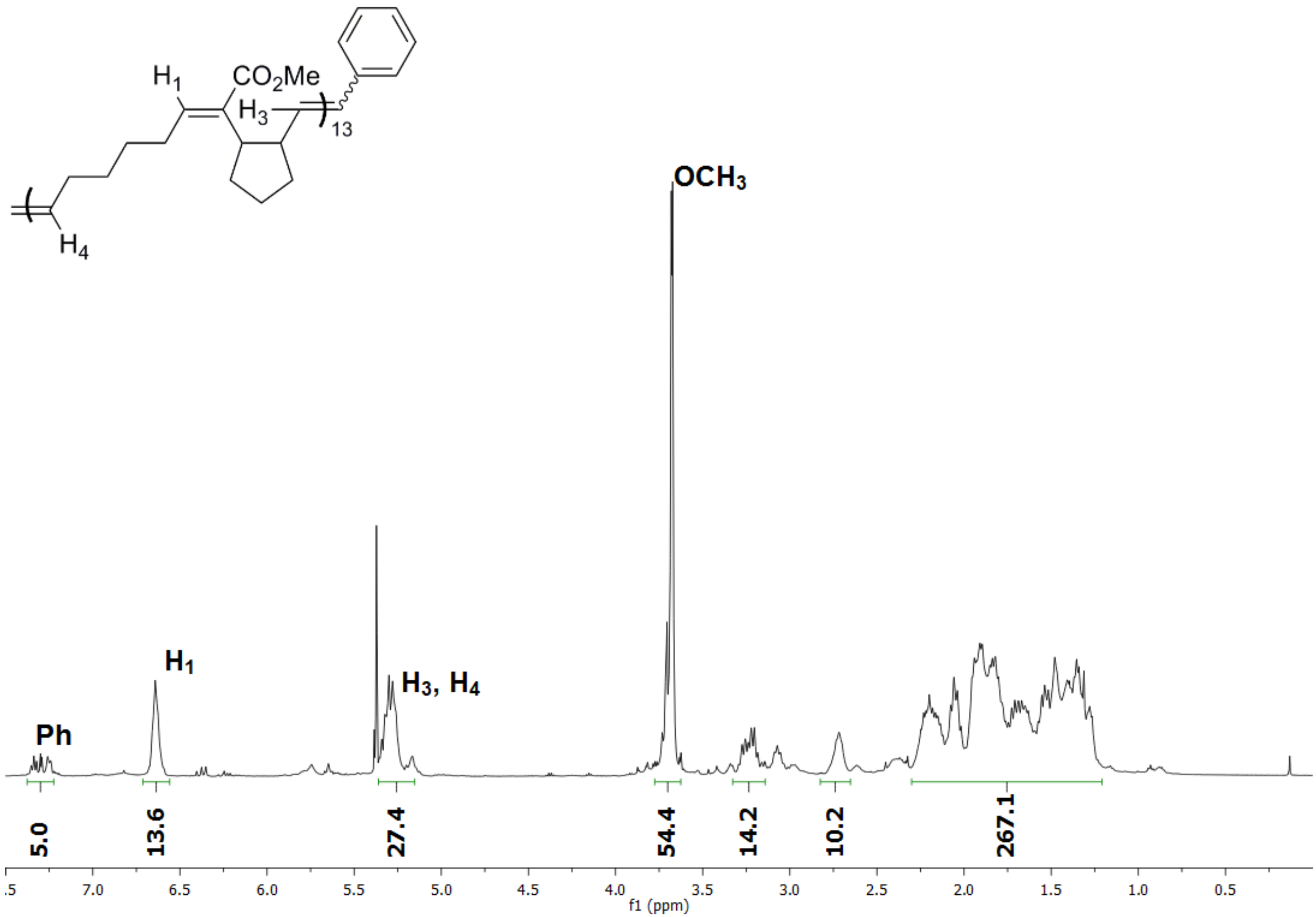

Figure S10. ^{1}H NMR spectrum of poly(**3**-*alt*-**6**)$_{13}$ in CD_2Cl_2.

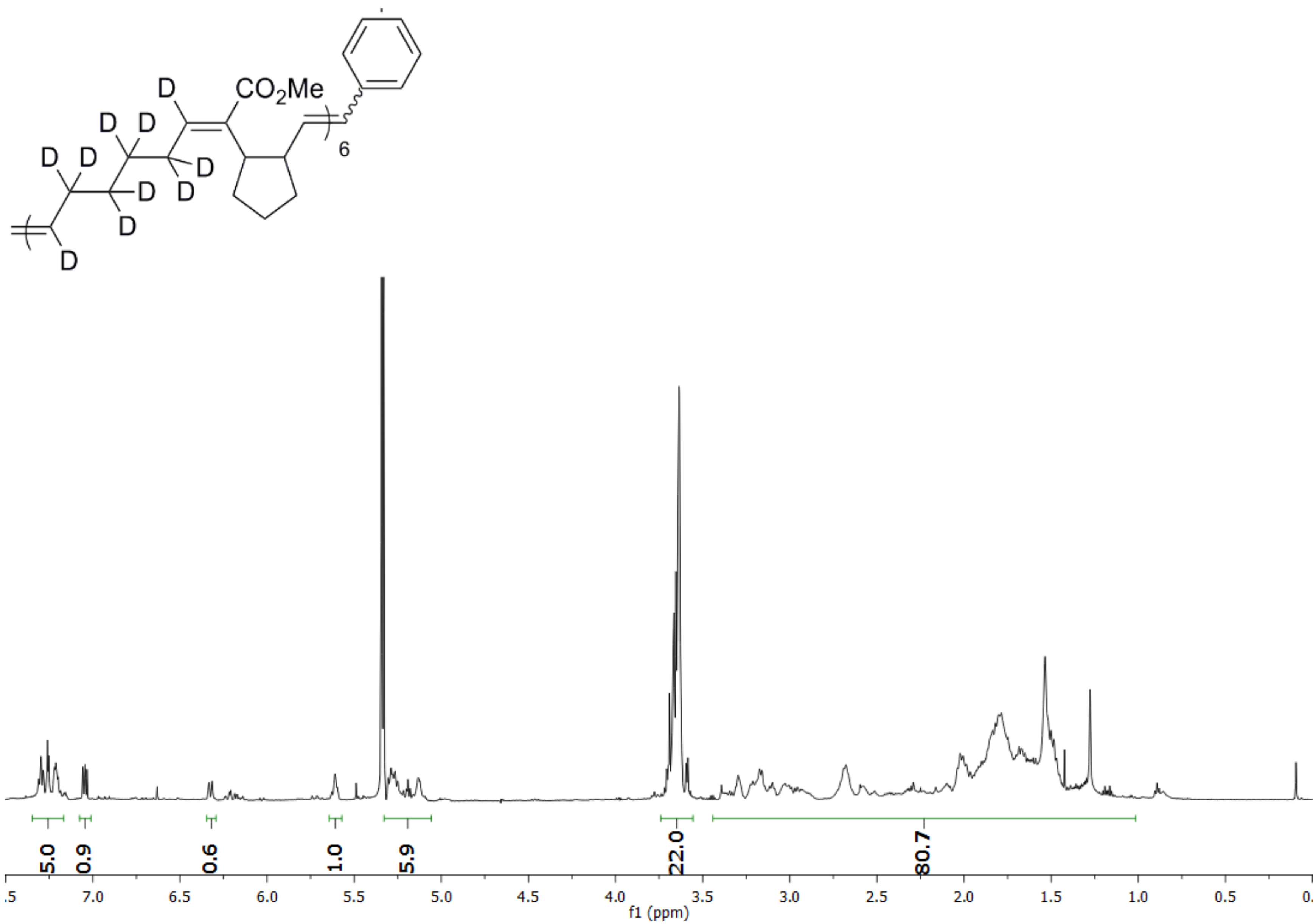

Figure S11. ^{1}H NMR spectrum of poly(**3**-*alt*-**6**-**d$_{10}$**)$_6$ in CD_2Cl_2.

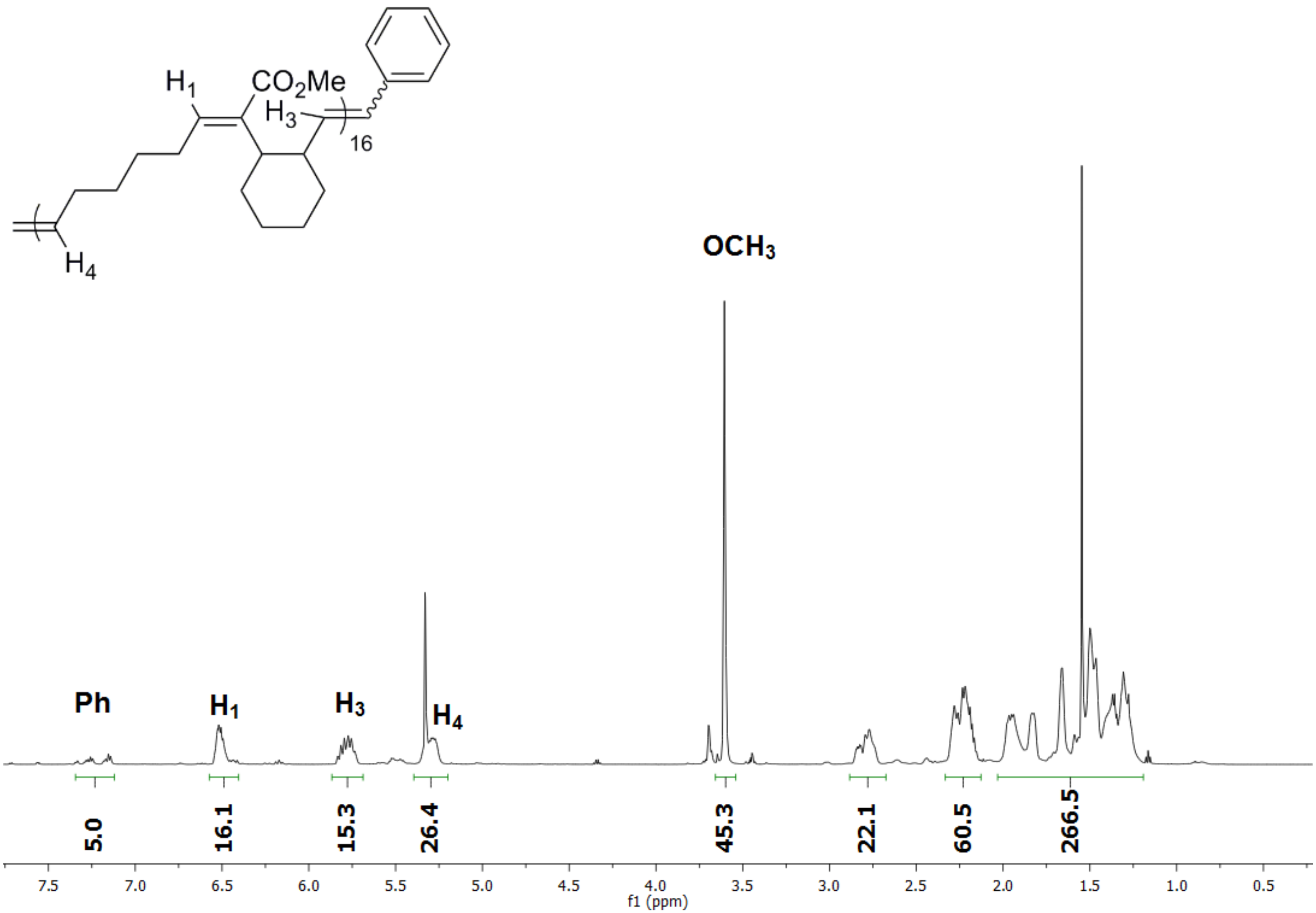

Figure S12. ^{1}H NMR spectrum of poly(**4**-*alt*-**6**)$_{16}$ obtained at 25 °C in CD_2Cl_2.

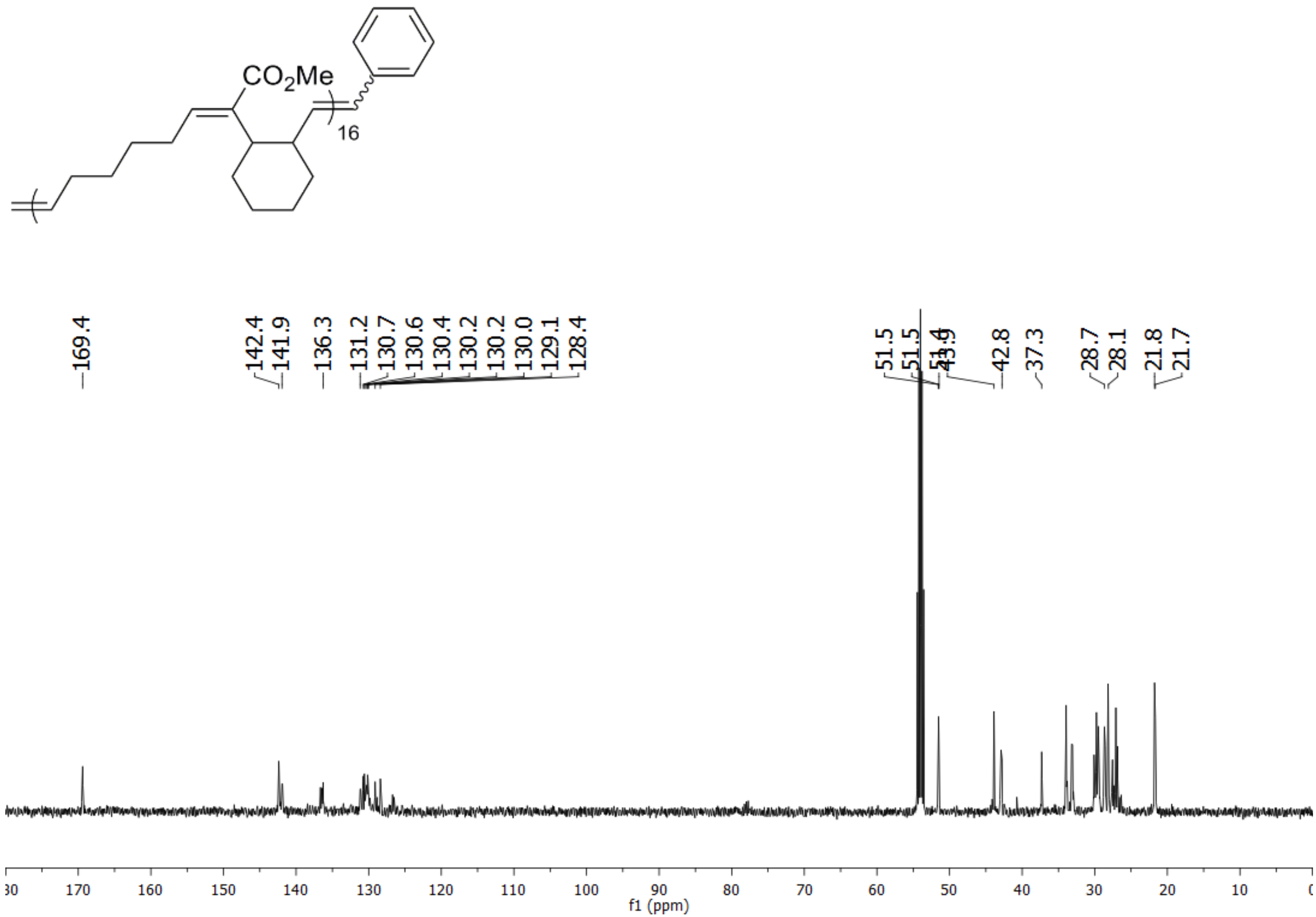

Figure S13. ^{13}C NMR spectrum of poly(**4**-*alt*-**6**)$_{16}$ obtained at 25 °C in CD_2Cl_2.

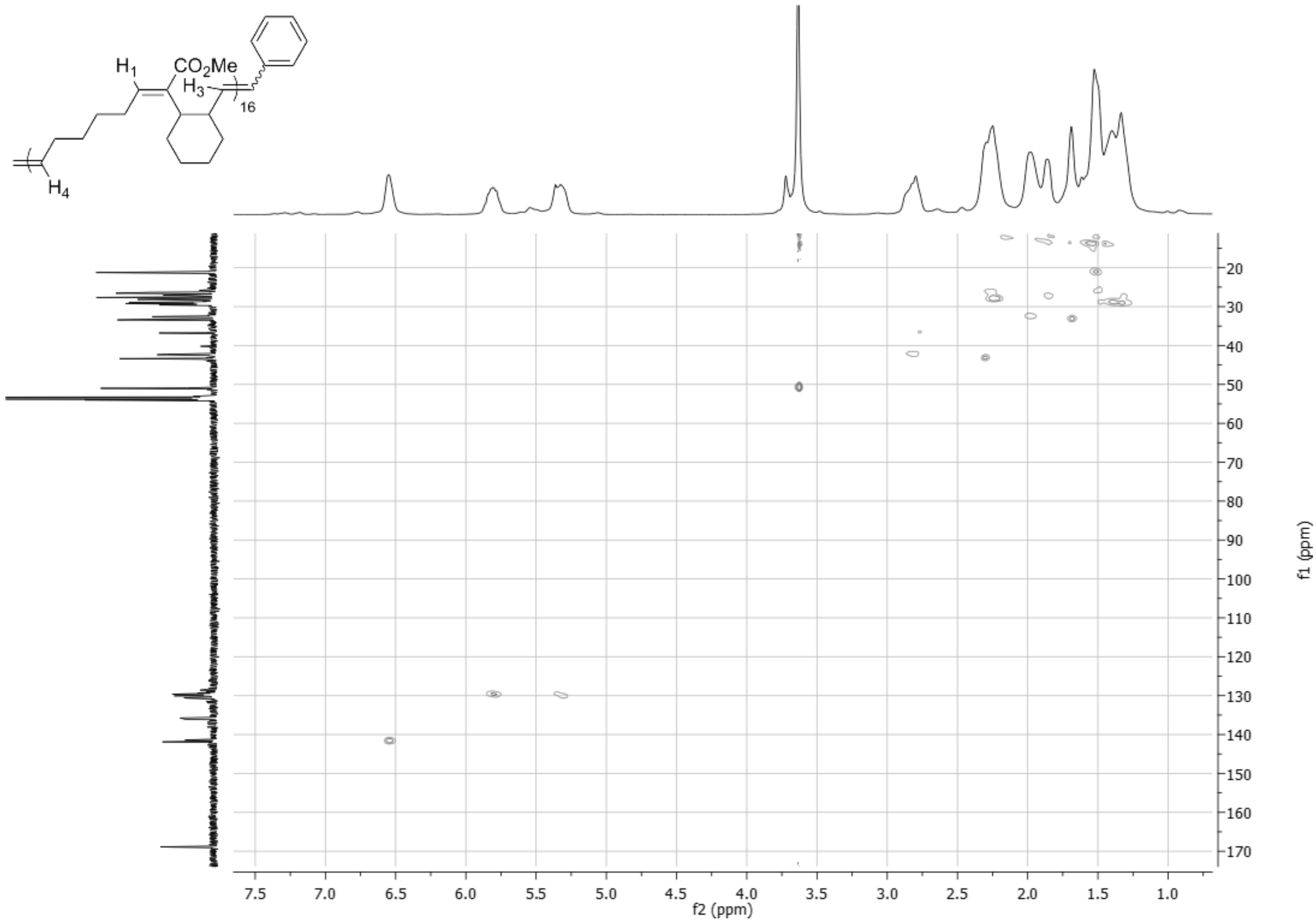

Figure S14. HSQC spectrum of poly(**4**-*alt*-**6**)$_{16}$ obtained at 25 °C in CD_2Cl_2.

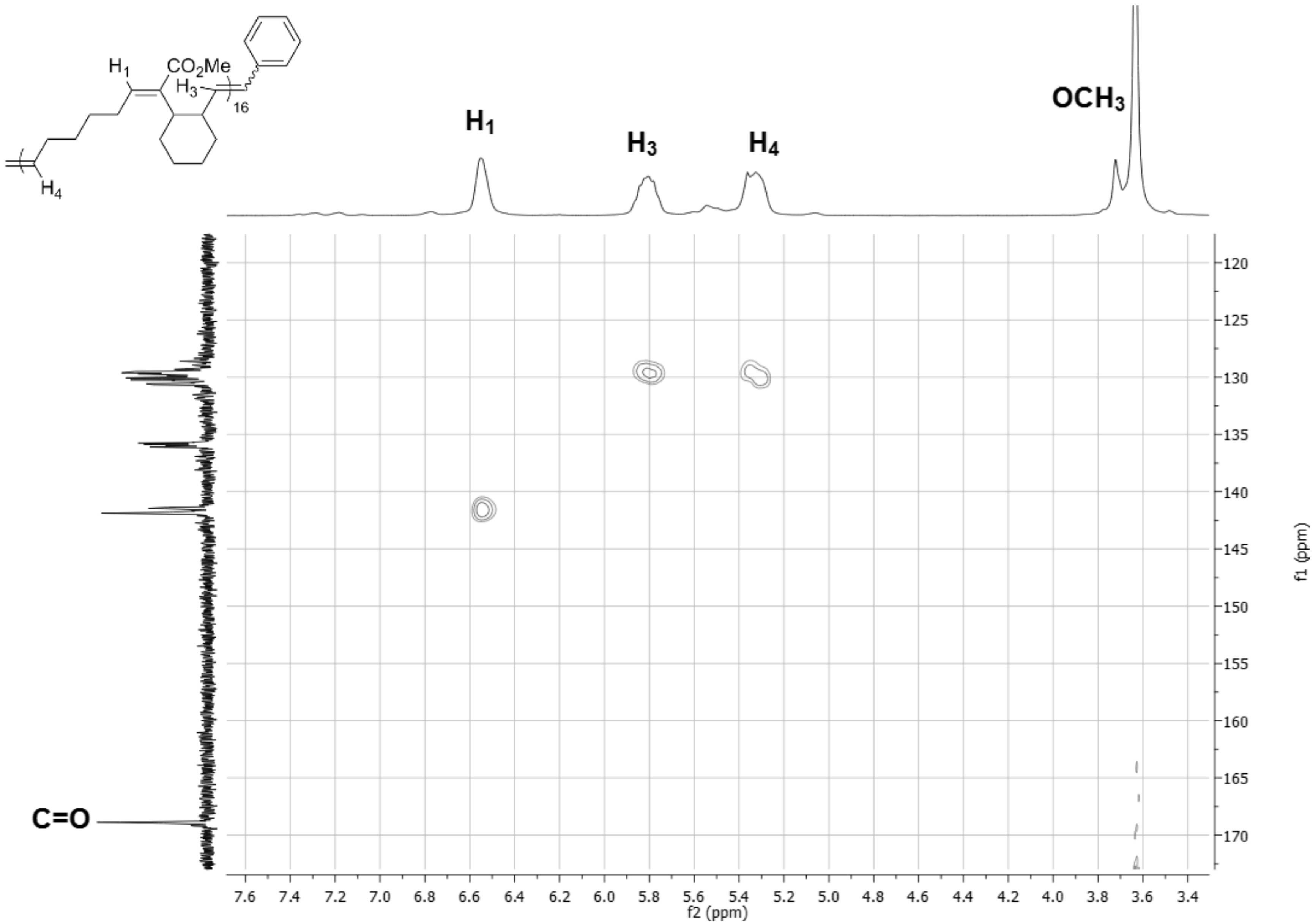

Figure S15. Alkene region of HSQC spectrum of poly(**4**-*alt*-**6**)$_{16}$ obtained at 25 °C in CD_2Cl_2.

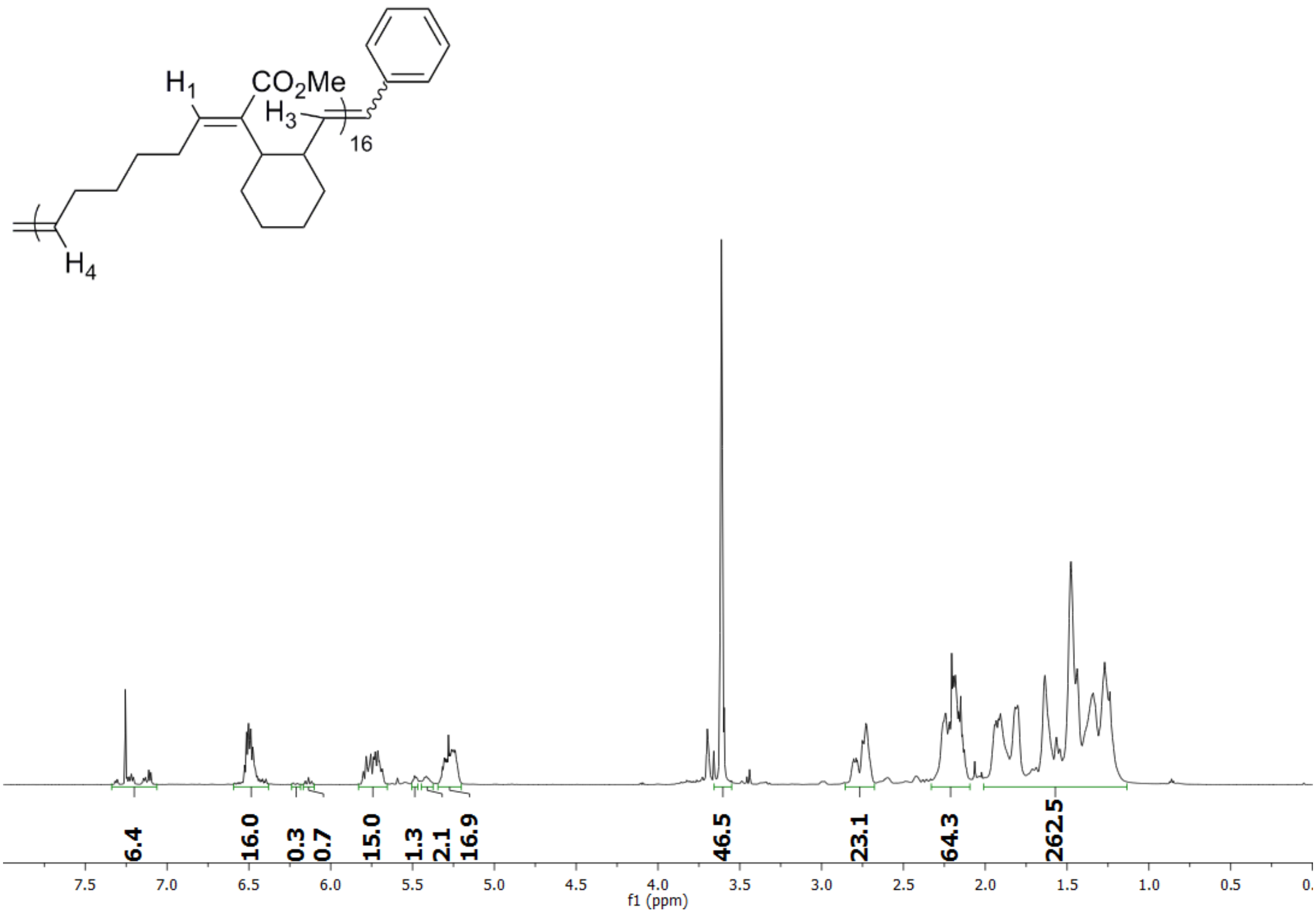

Figure S16. ^{1}H NMR spectrum of poly(**4**-*alt*-**6**)$_{16}$ obtained at 35 °C in $CDCl_3$.

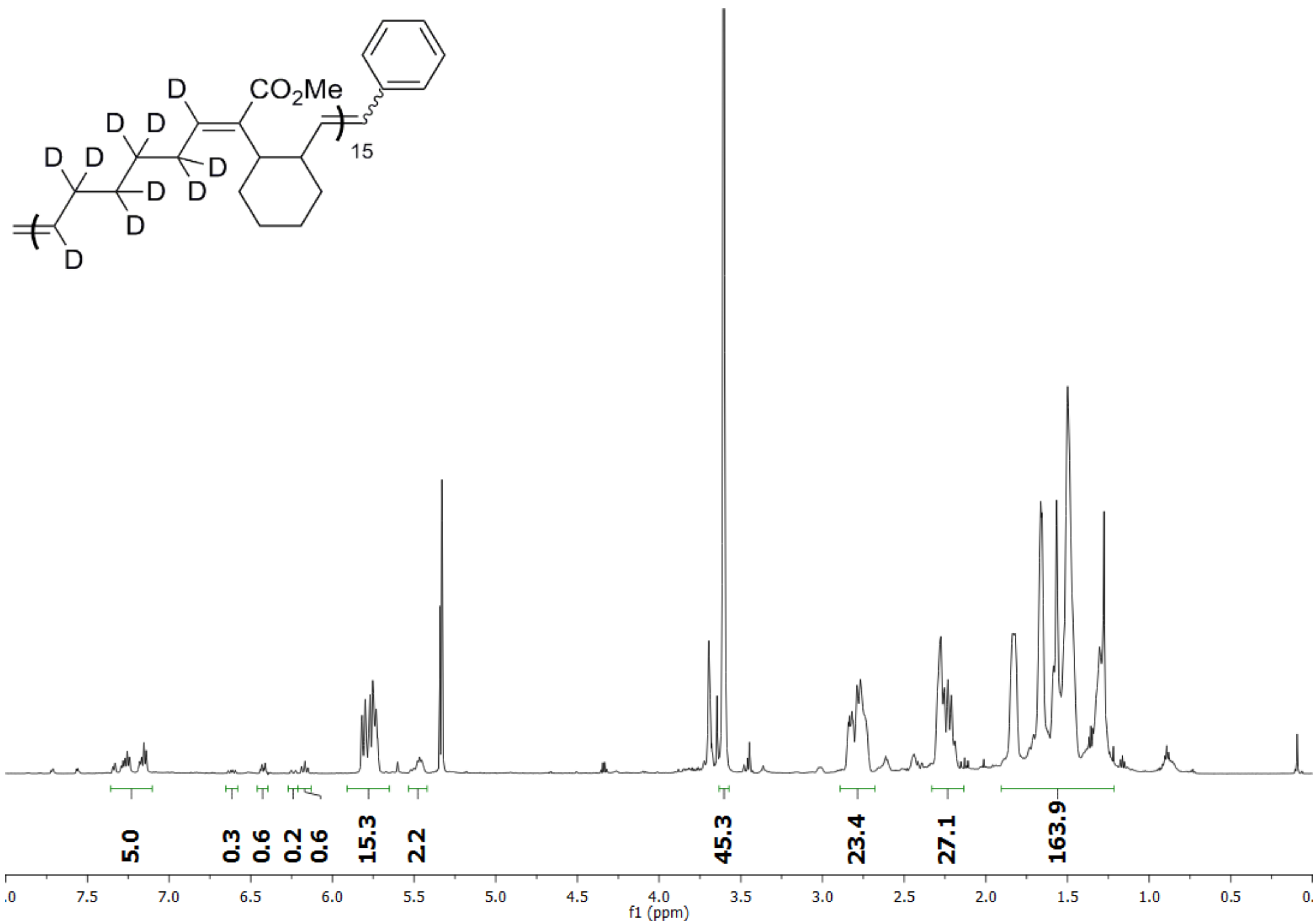

Figure S17. ^{1}H NMR spectrum of poly(**4**-*alt*-**6-d$_{10}$**)$_{15}$ in CD_2Cl_2.

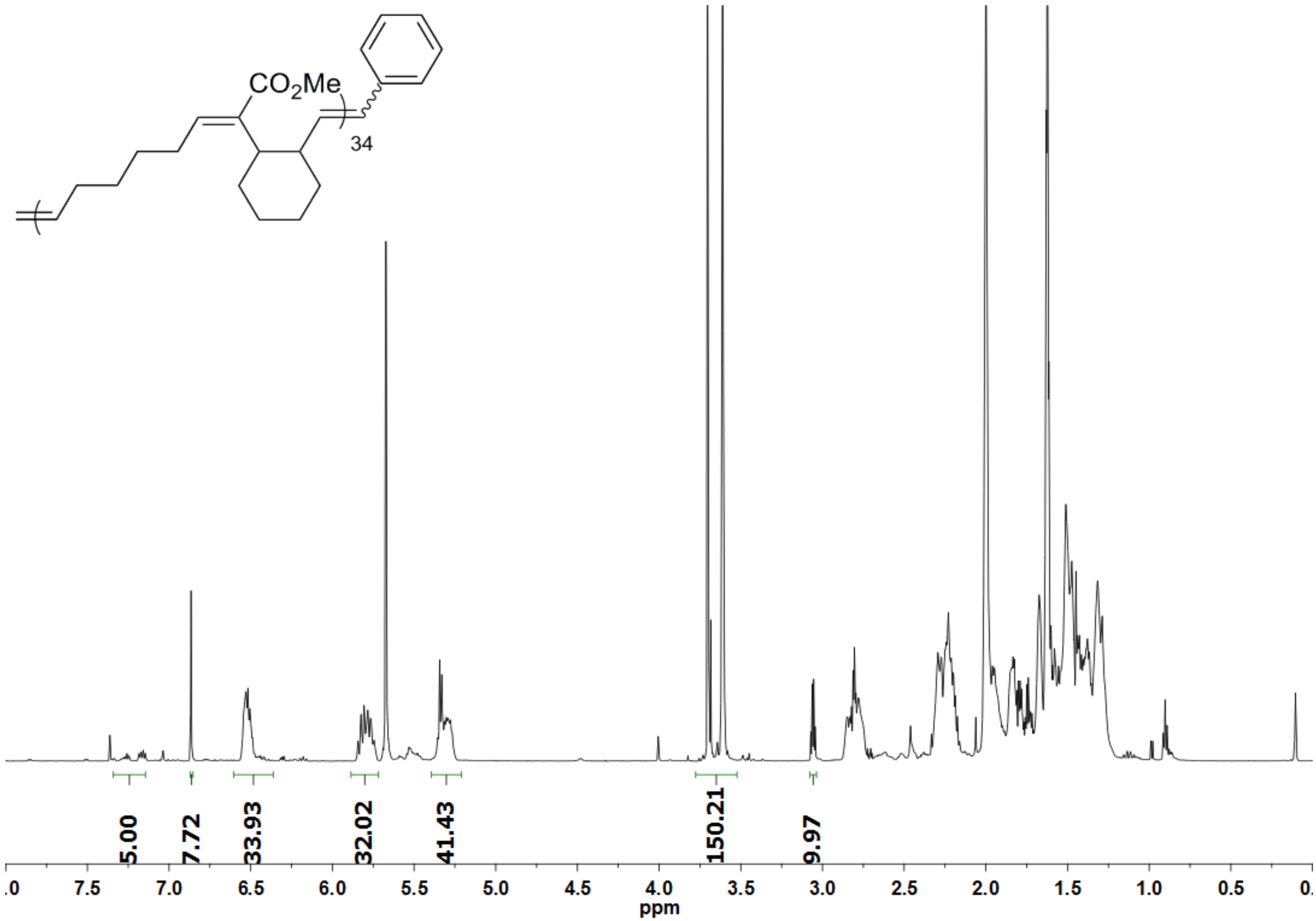

Figure S18. [1]H NMR spectrum of crude poly(**4**-*alt*-**6**)$_{34}$ obtained at 35 °C in CD_2Cl_2.

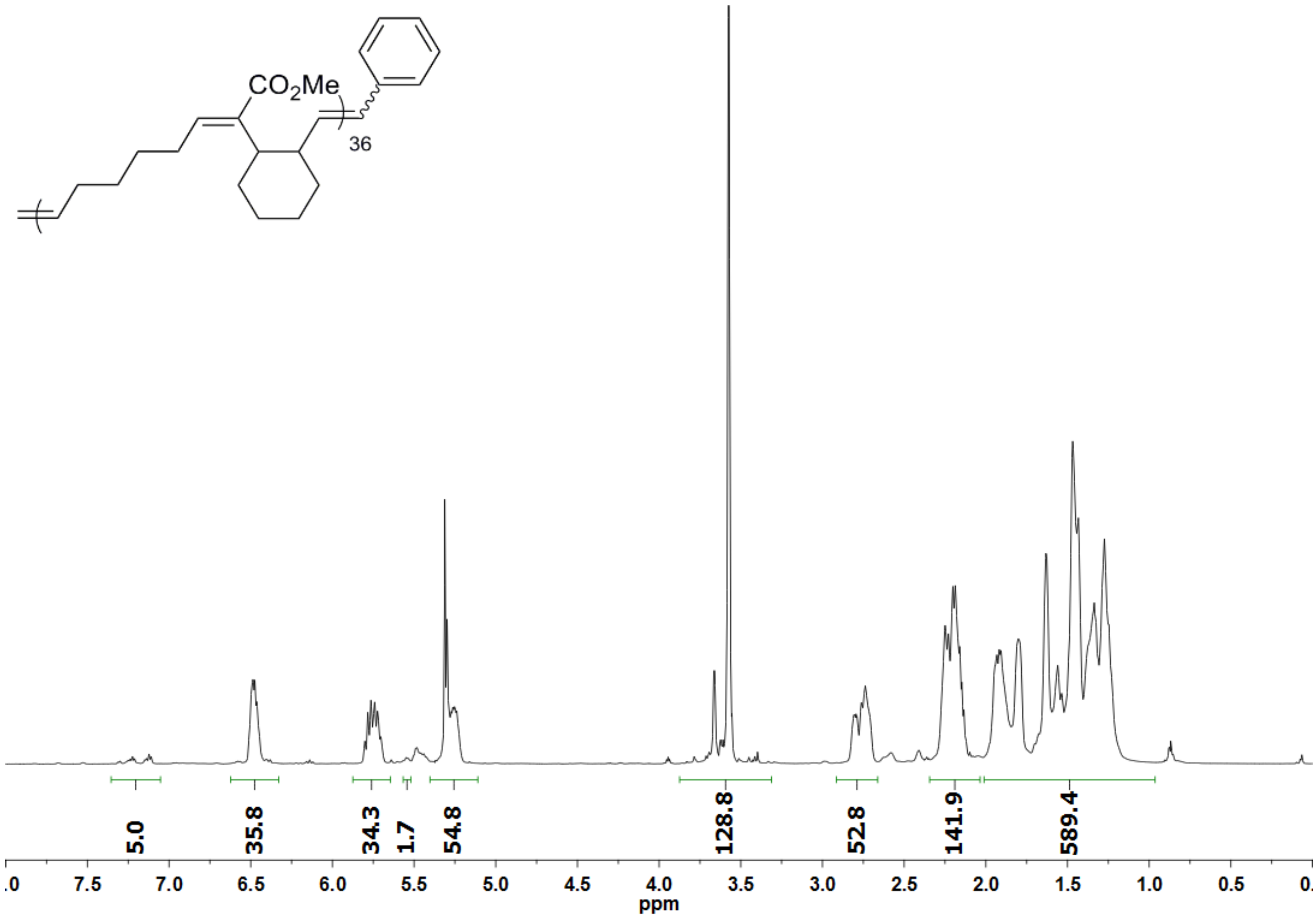

Figure S19. ^{1}H NMR spectrum of poly(**4**-*alt*-**6**)$_{36}$ obtained at 60 °C in CD_2Cl_2.

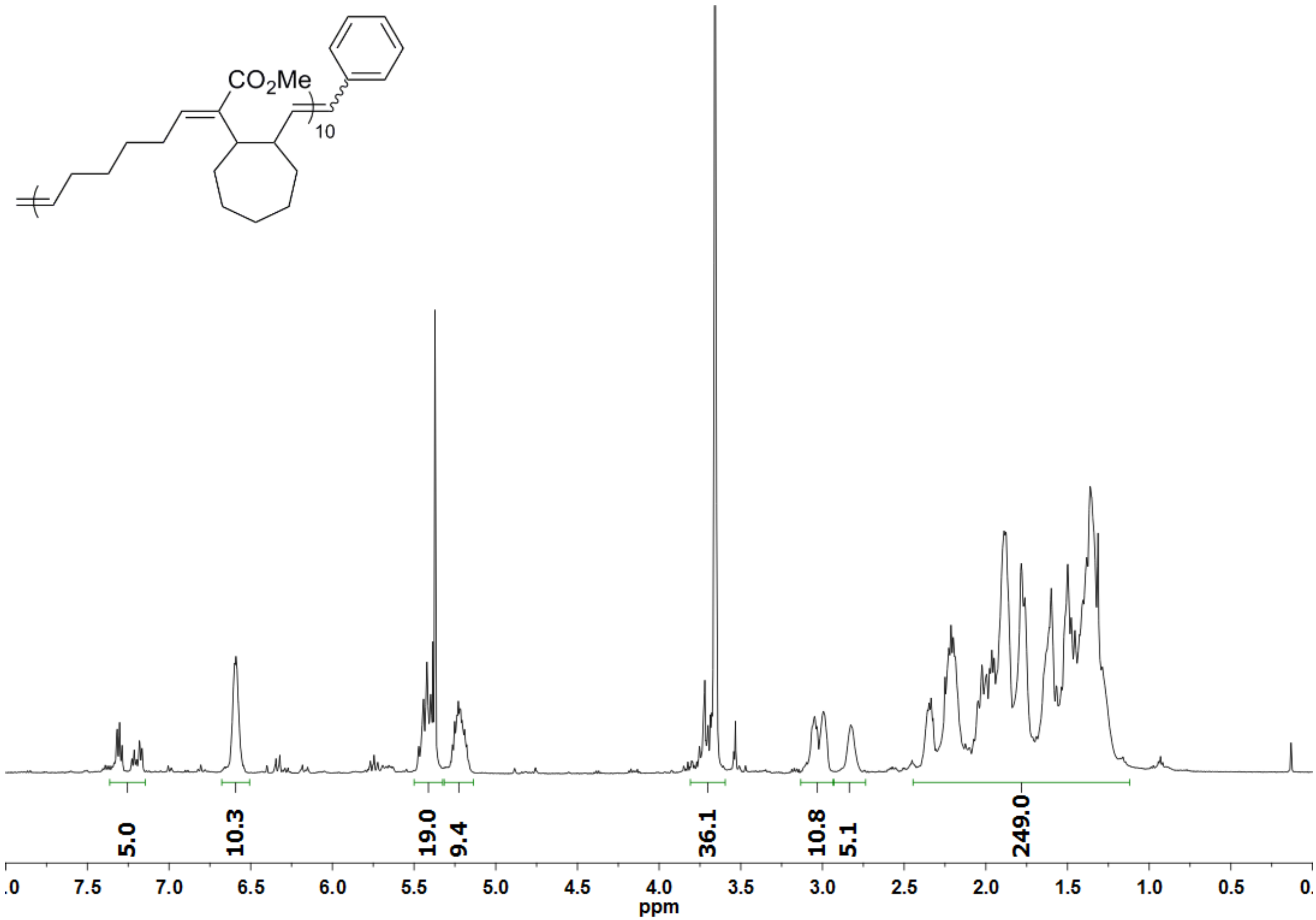

Figure S20. ^{1}H NMR spectrum of poly(**5**-*alt*-**6**)$_{10}$ in CD_2Cl_2.

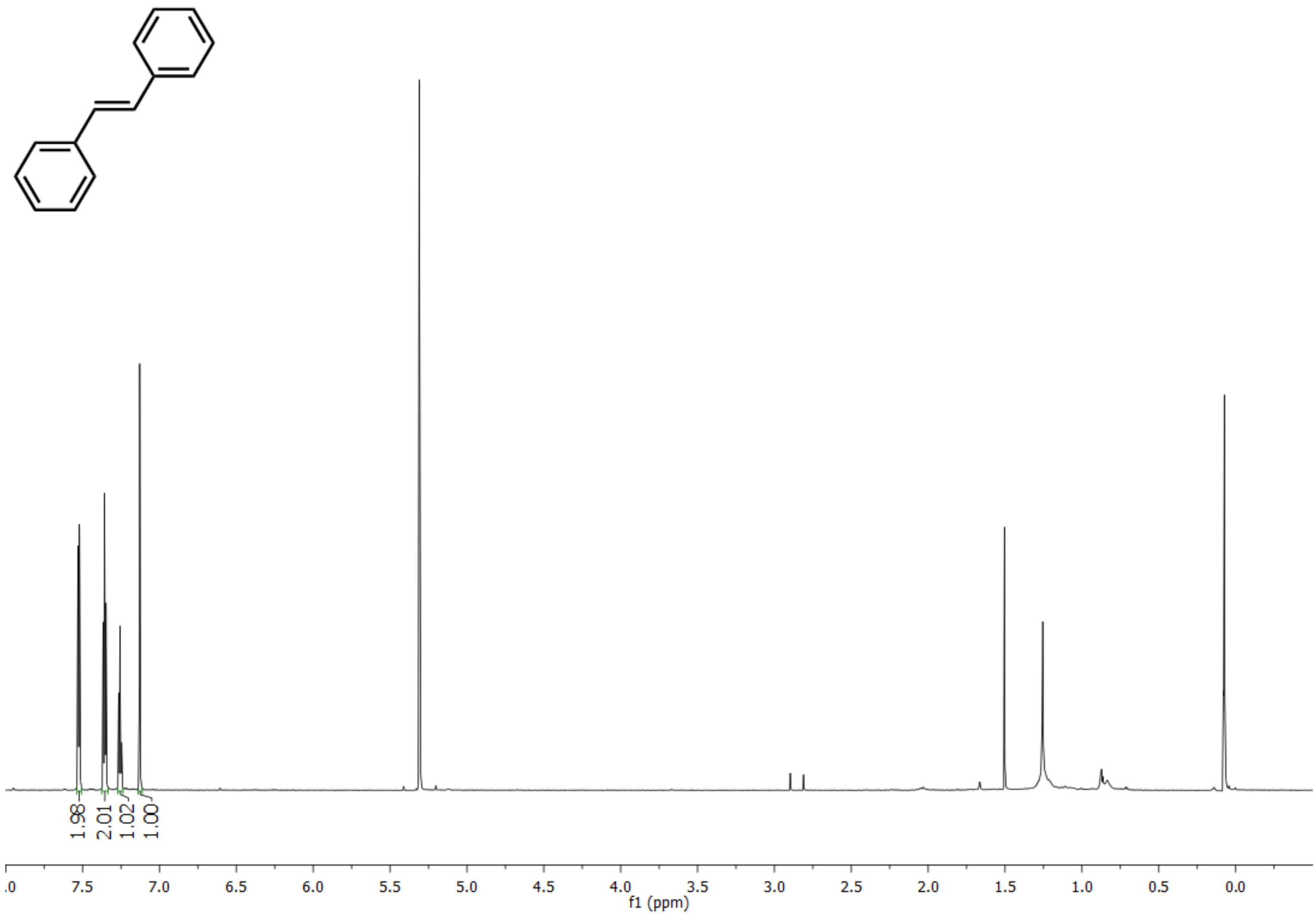

Figure S21. [1]H NMR spectrum of *E*-stilbene in CD_2Cl_2.

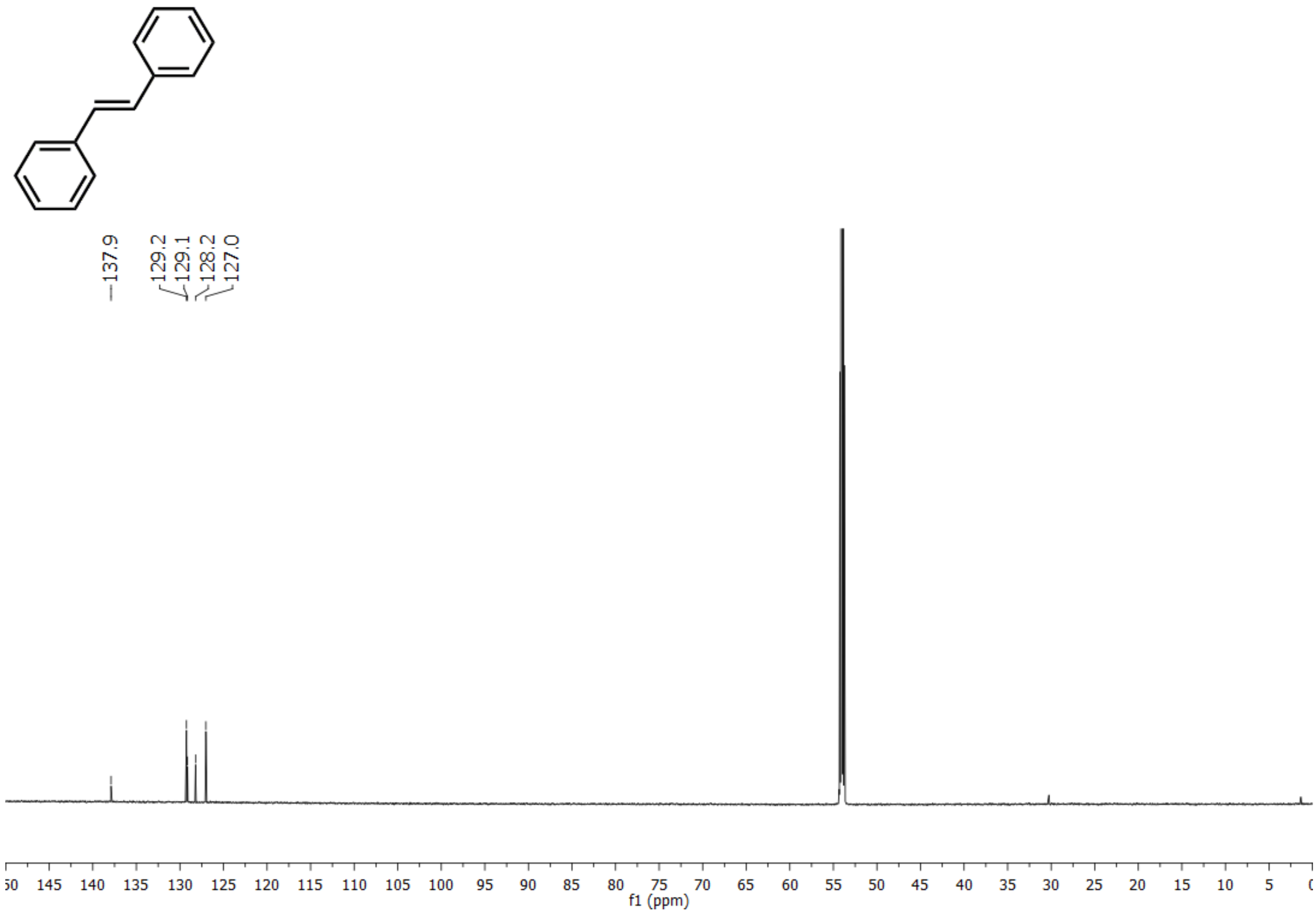

Figure S22. ^{13}C NMR spectrum of *E*-stilbene in CD_2Cl_2 (fraction I).

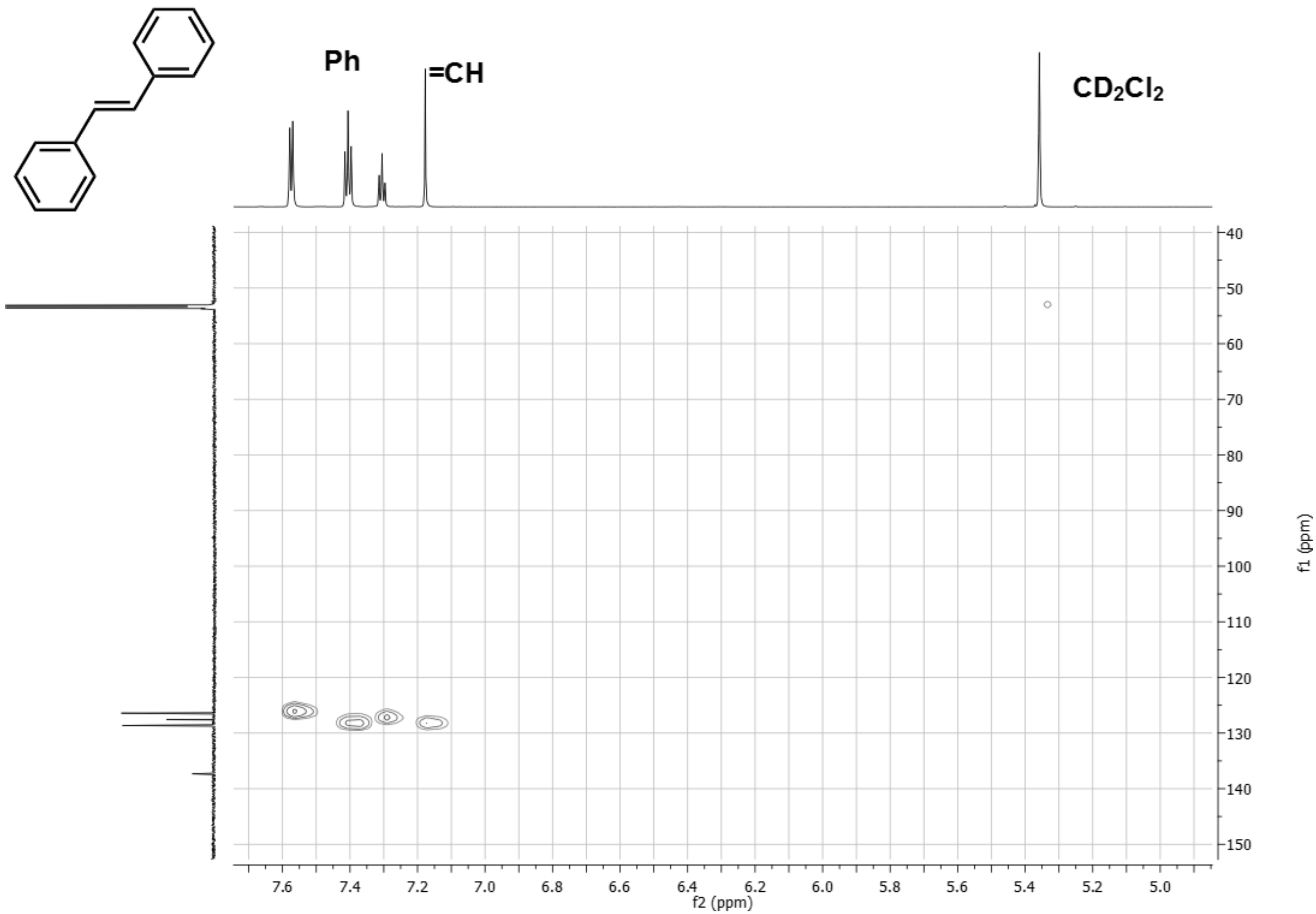

Figure S23. HSQC spectrum of *E*-stilbene in CD_2Cl_2 (fraction I).

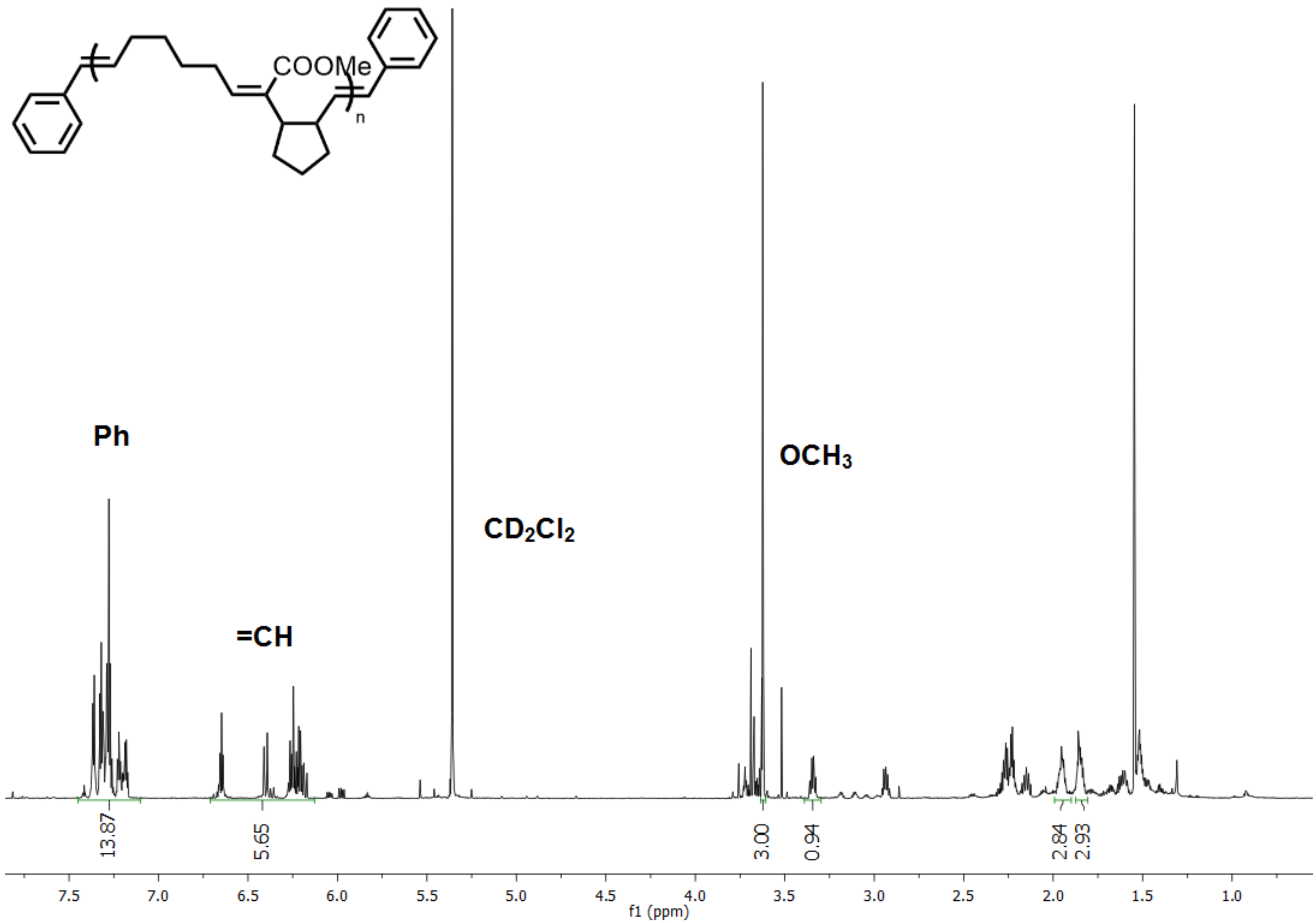

Figure S24. ^{1}H NMR spectrum of partially purified Ph-(**3**-*alt*-**6**)-Ph in CD_2Cl_2 (fraction II).

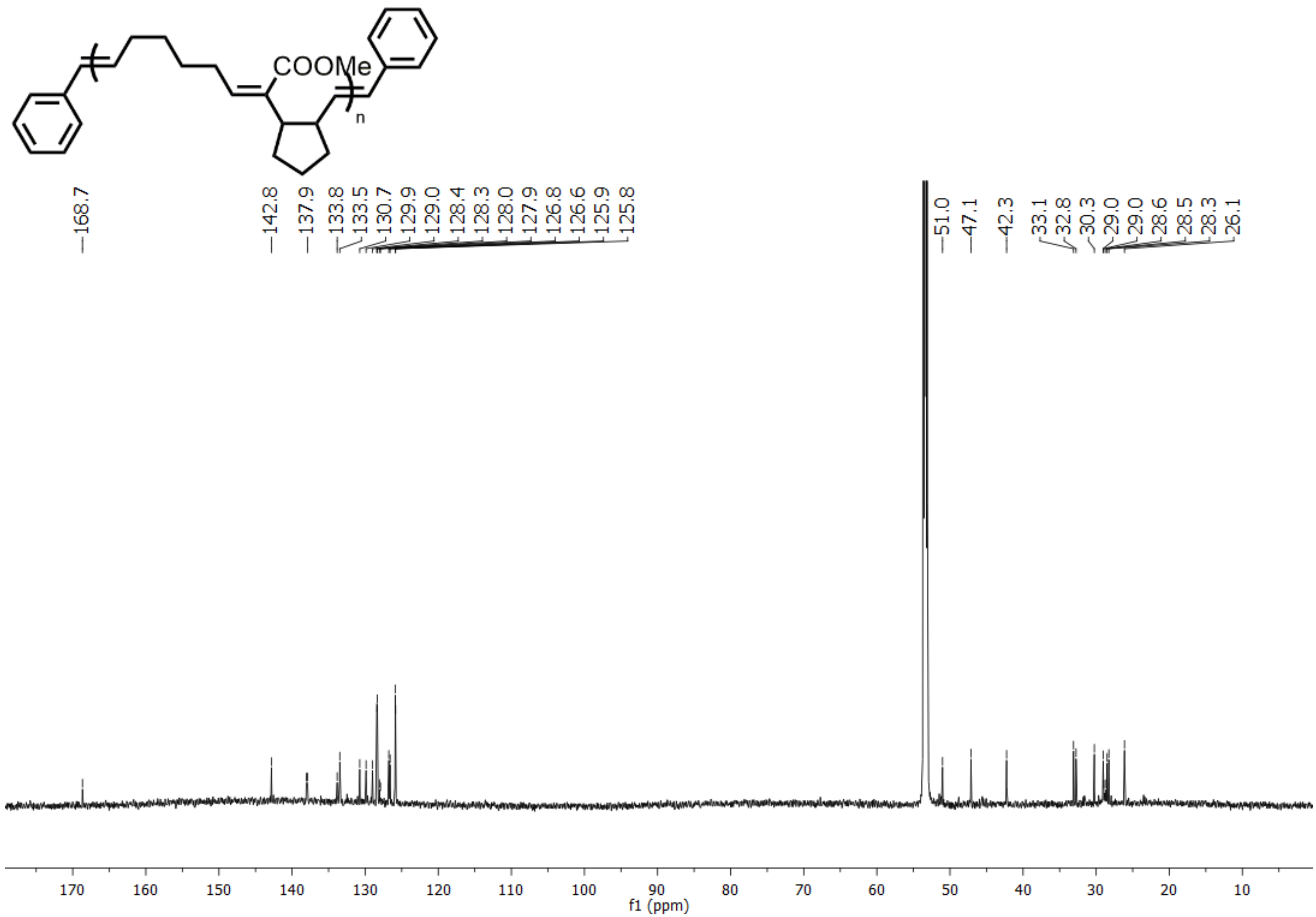

Figure S25. ^{13}C NMR spectrum of partially purified Ph-(**3**-*alt*-**6**)-Ph in CD_2Cl_2 (fraction II).

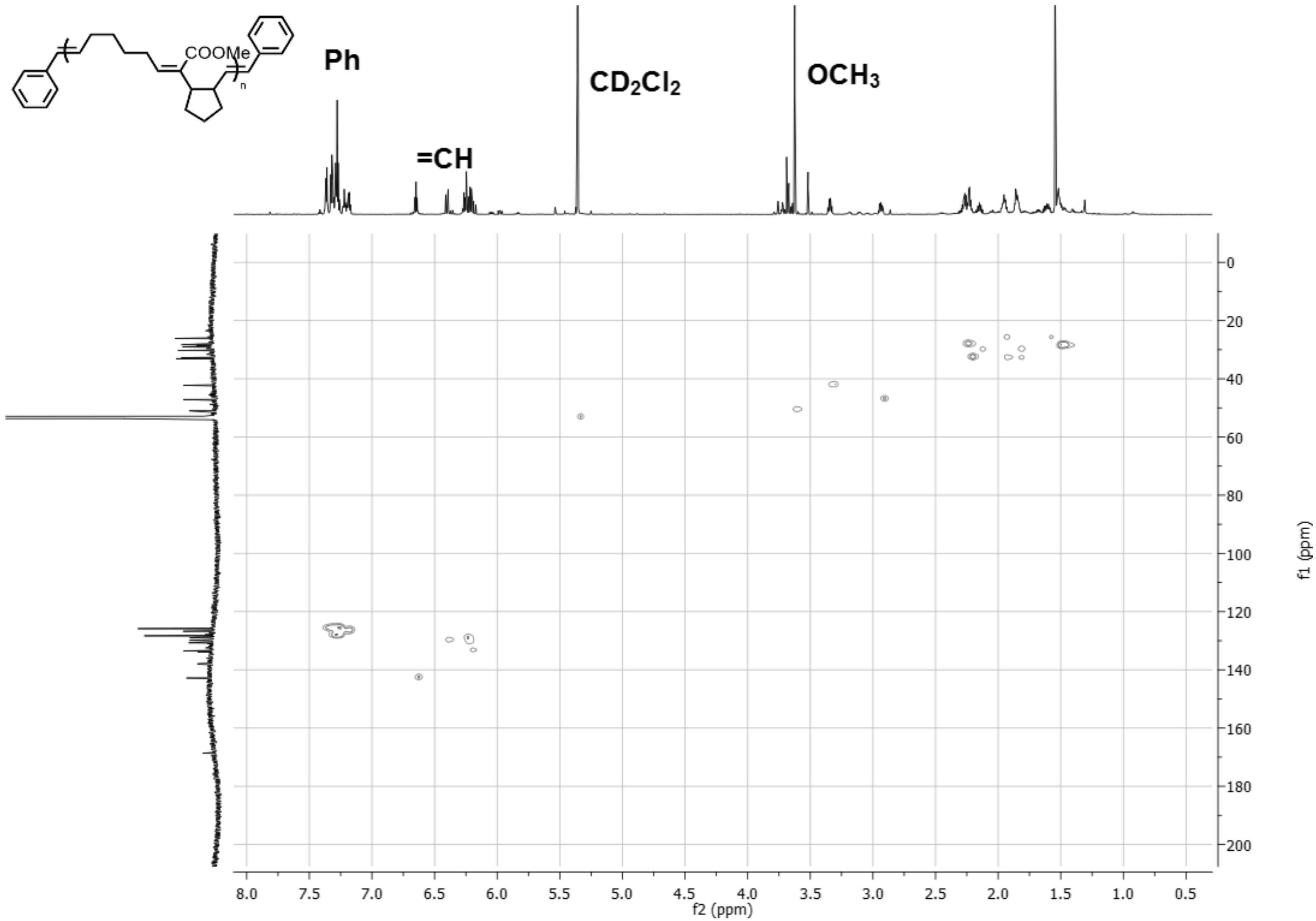

Figure S26. [1]H NMR spectrum of partially purified Ph-(**3**-*alt*-**6**)-Ph in CD_2Cl_2 (fraction II).

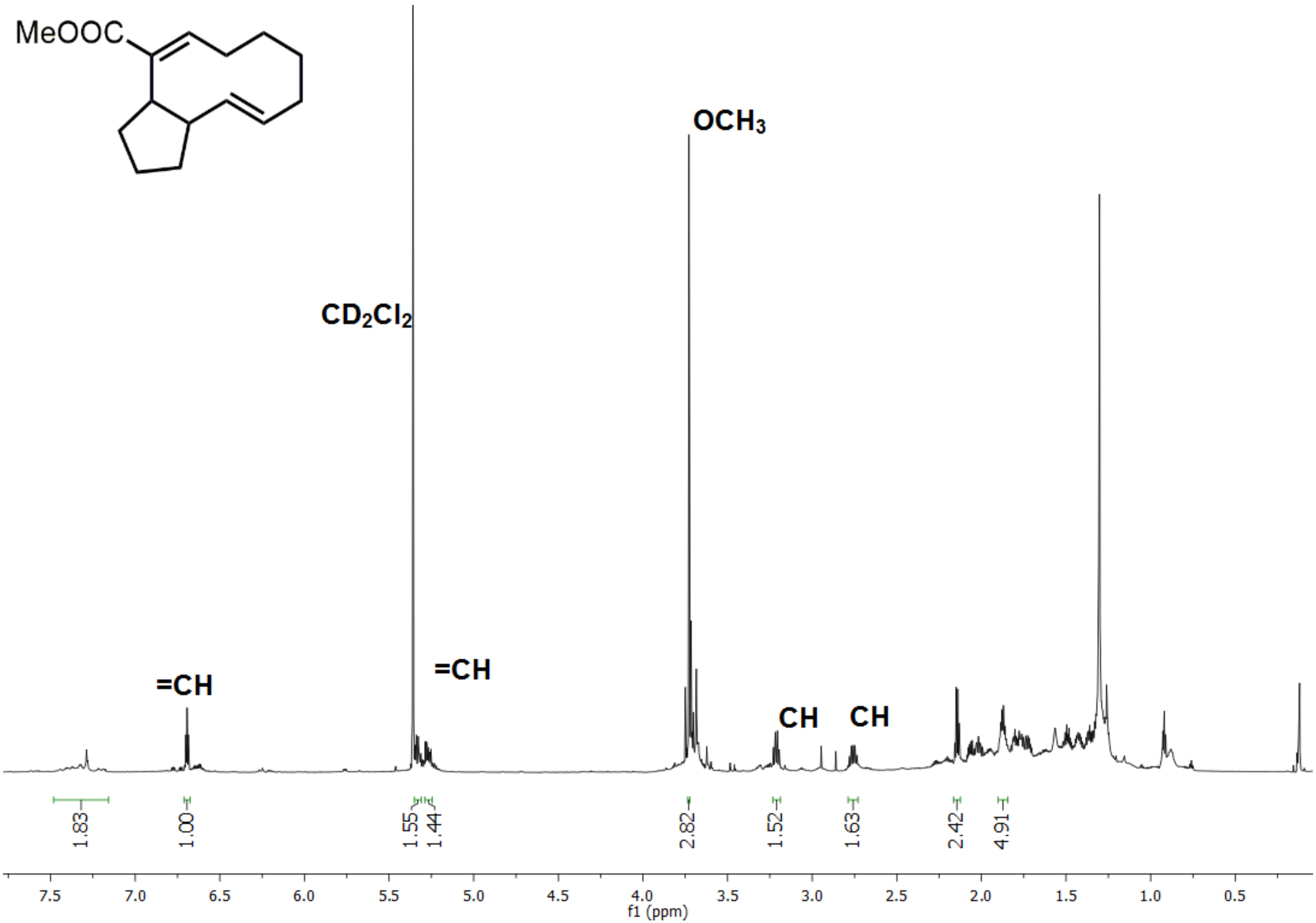

Figure S27. ^{1}H NMR spectrum of partially purified *cyc*-(**3**-*alt*-**6**)$_1$ in CD_2Cl_2 (fraction III).

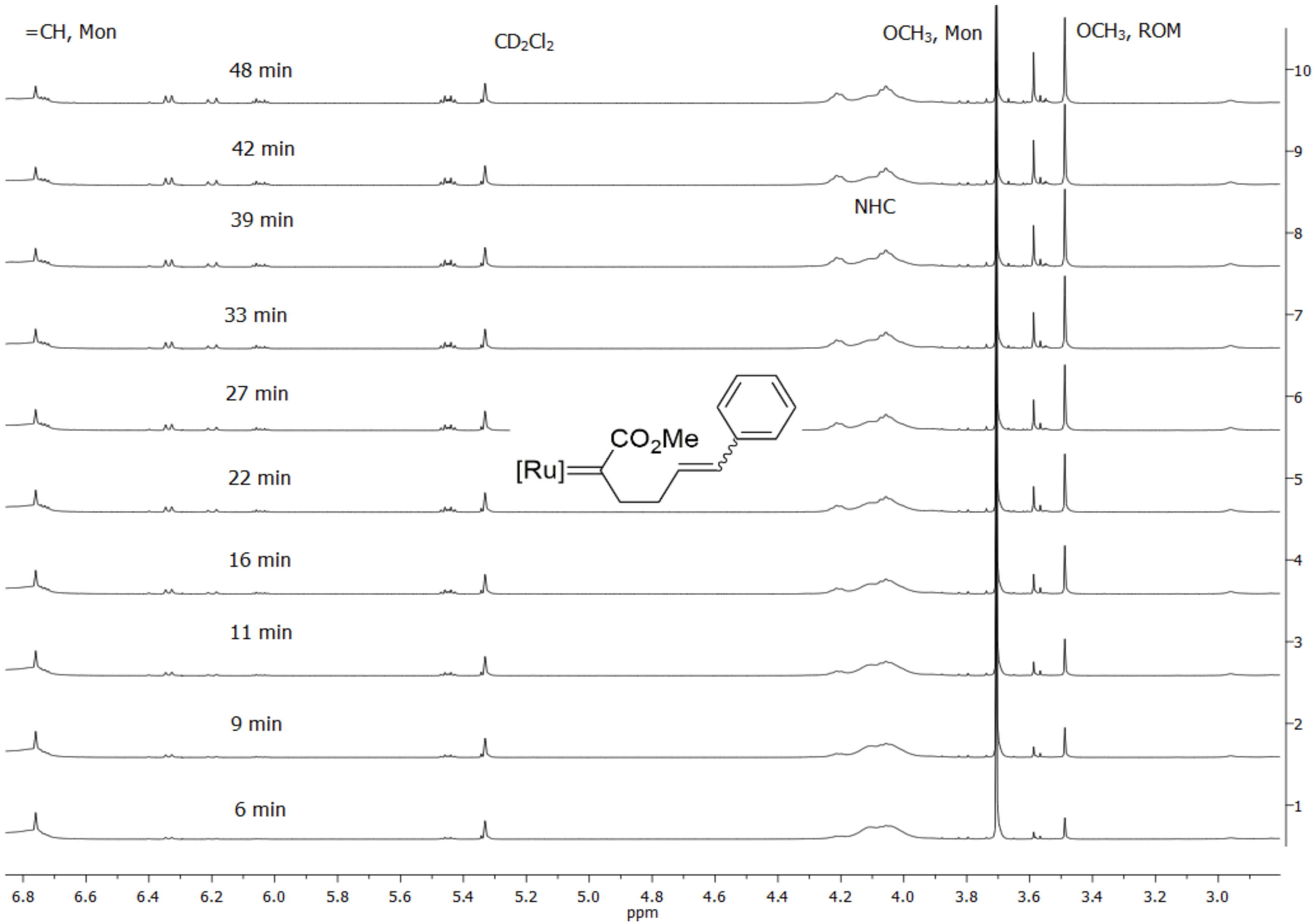

Figure S28. ROM of monomer **1** in CD_2Cl_2 monitored by ^1H NMR spectroscopy as a function of time.

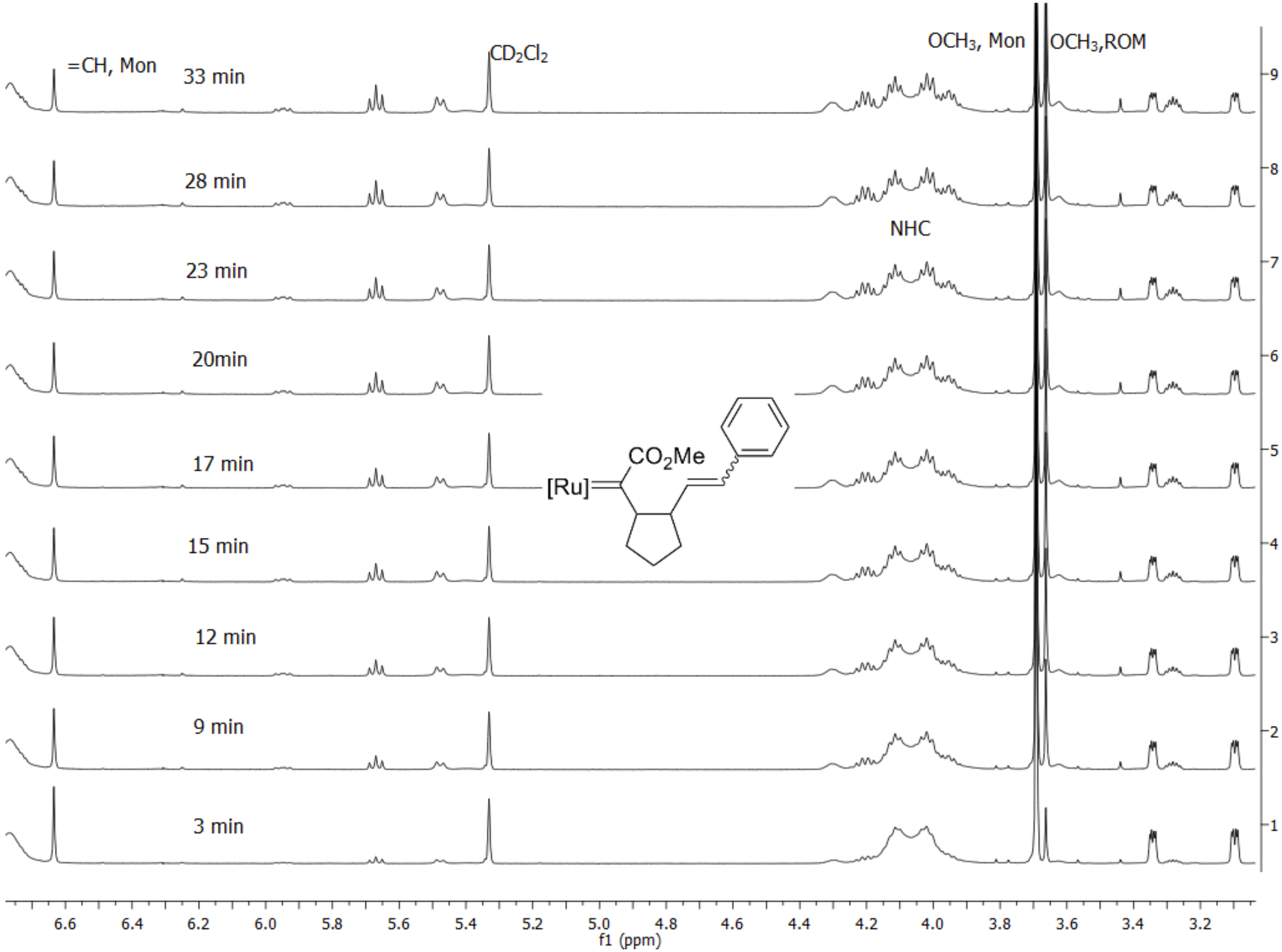

Figure S29. ROM of monomer **3** in CD_2Cl_2 monitored by ^1H NMR spectroscopy as a function of time.

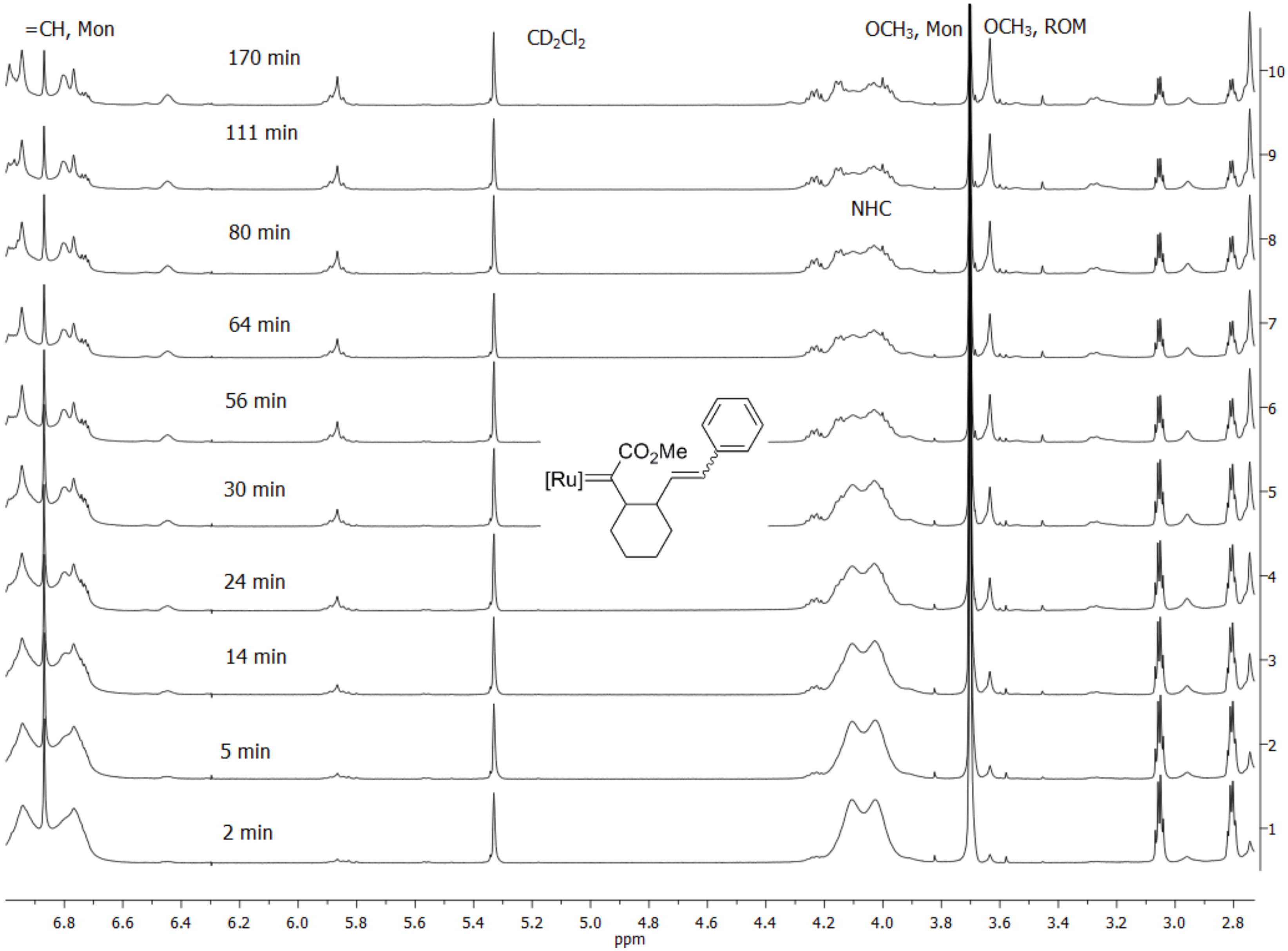

Figure S30. ROM of monomer **4** in CD_2Cl_2 monitored by ^1H NMR spectroscopy as a function of time.

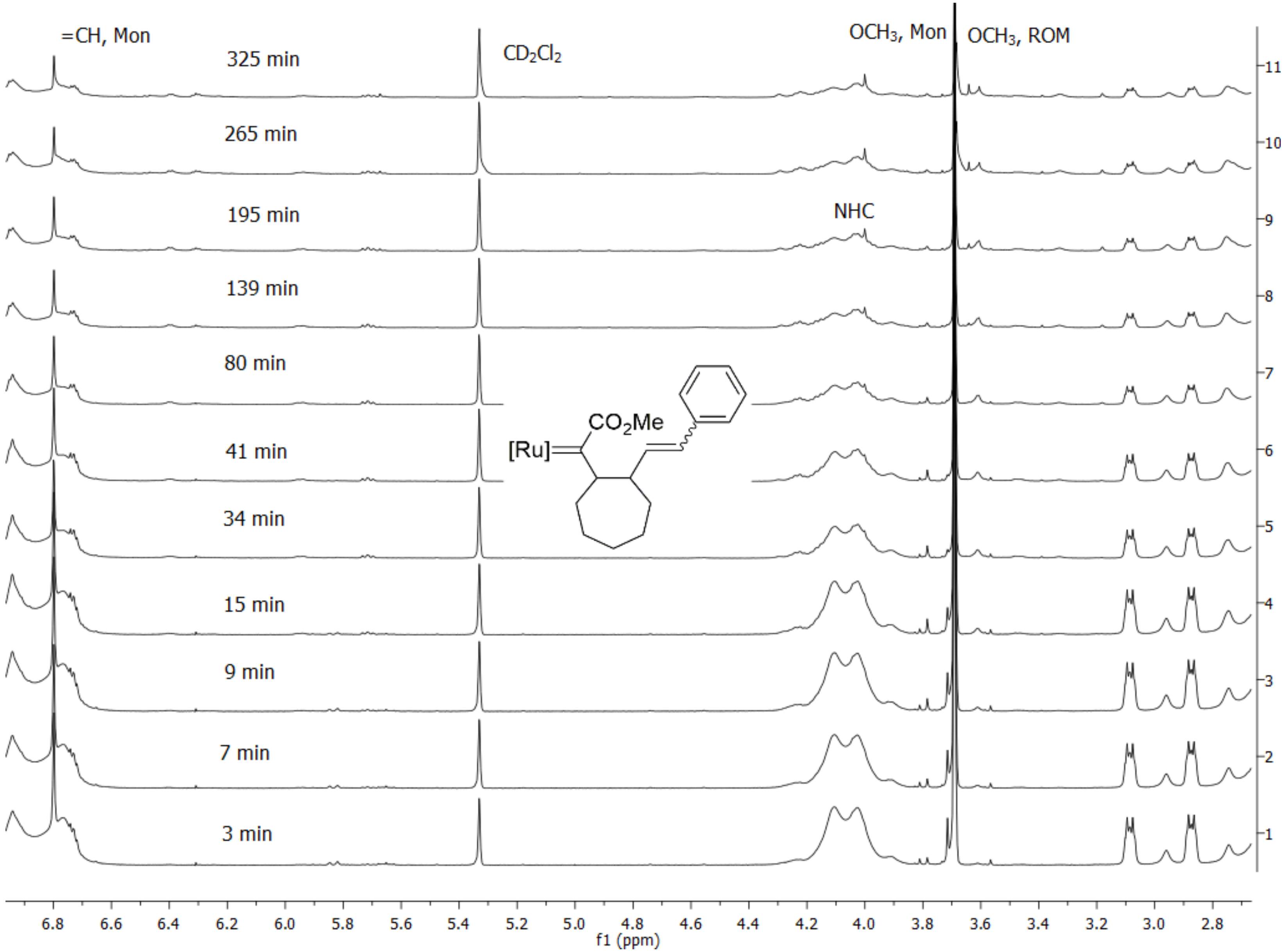

Figure S31. ROM of monomer **5** in CD_2Cl_2 monitored by ^1H NMR spectroscopy as a function of time.

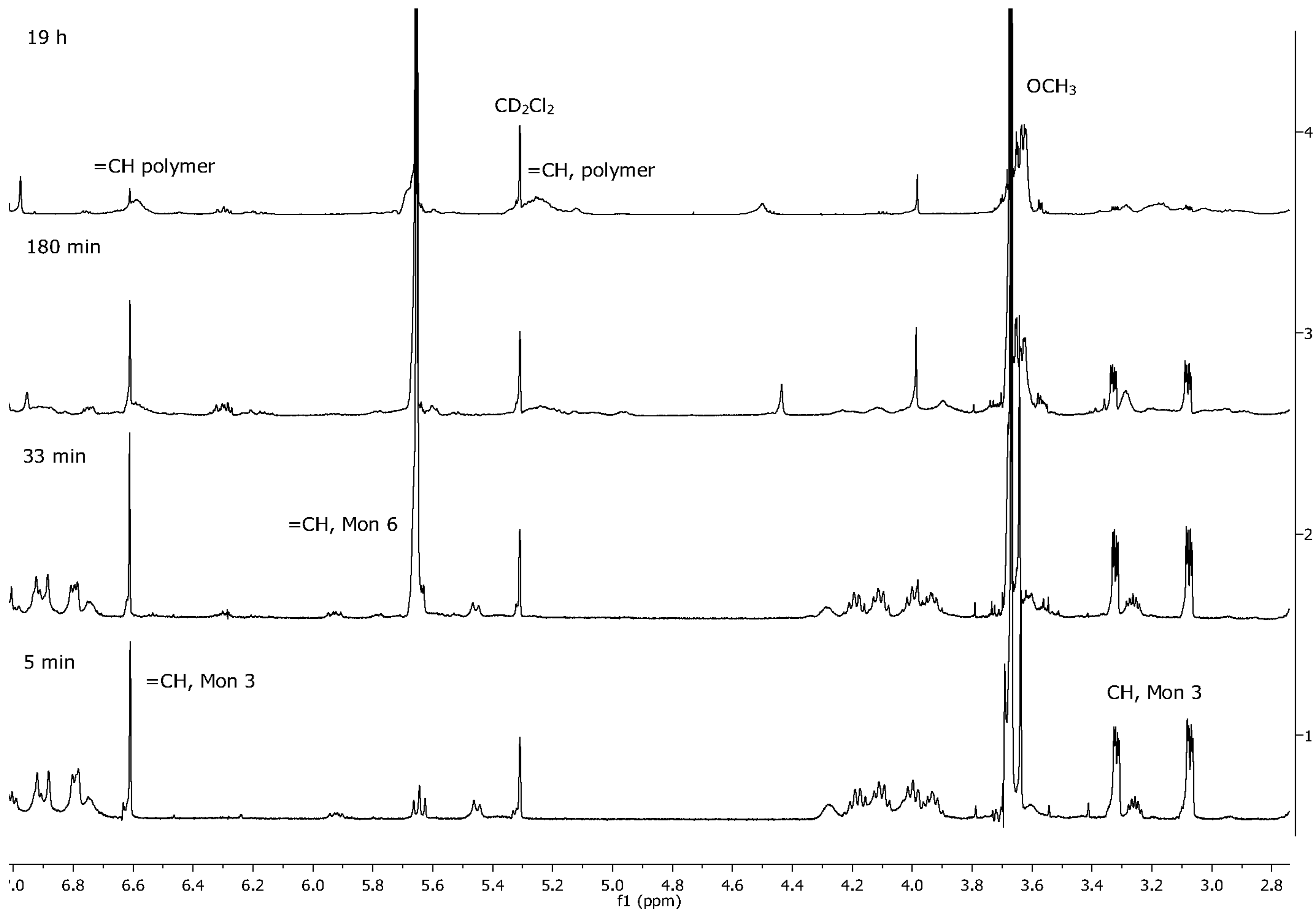

Figure S32. AROMP of monomer **3** and cyclohexene **6** ([**Ru**]:**3**:**6**=1:25:50) in CD_2Cl_2 monitored by ^1H NMR spectroscopy as a function of time.

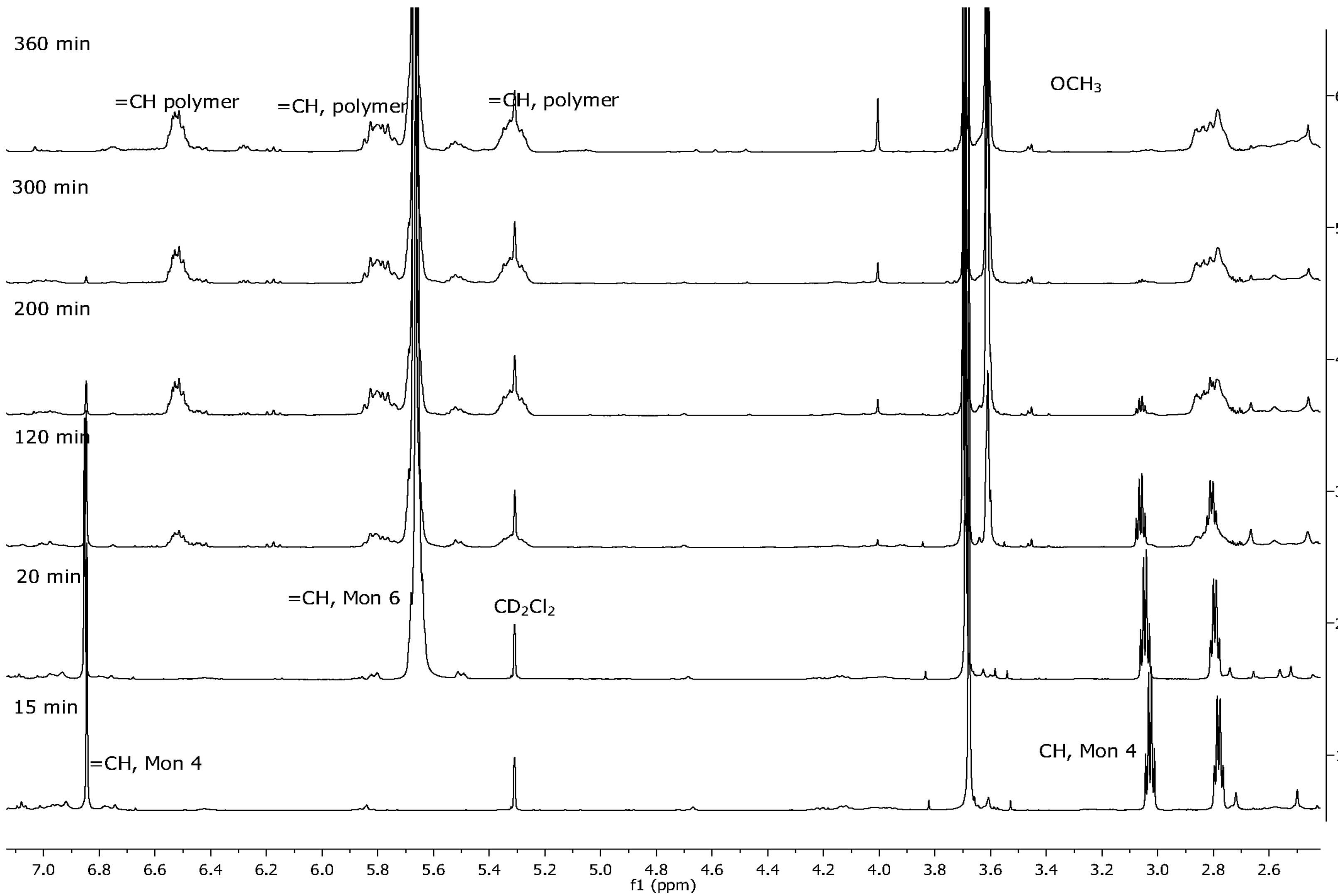

Figure S33. AROMP of monomer **4** and cyclohexene **6** ([**Ru**]:**4**:**6**=1:20:40) in CD_2Cl_2 monitored by ^{1}H NMR spectroscopy as a function of time.

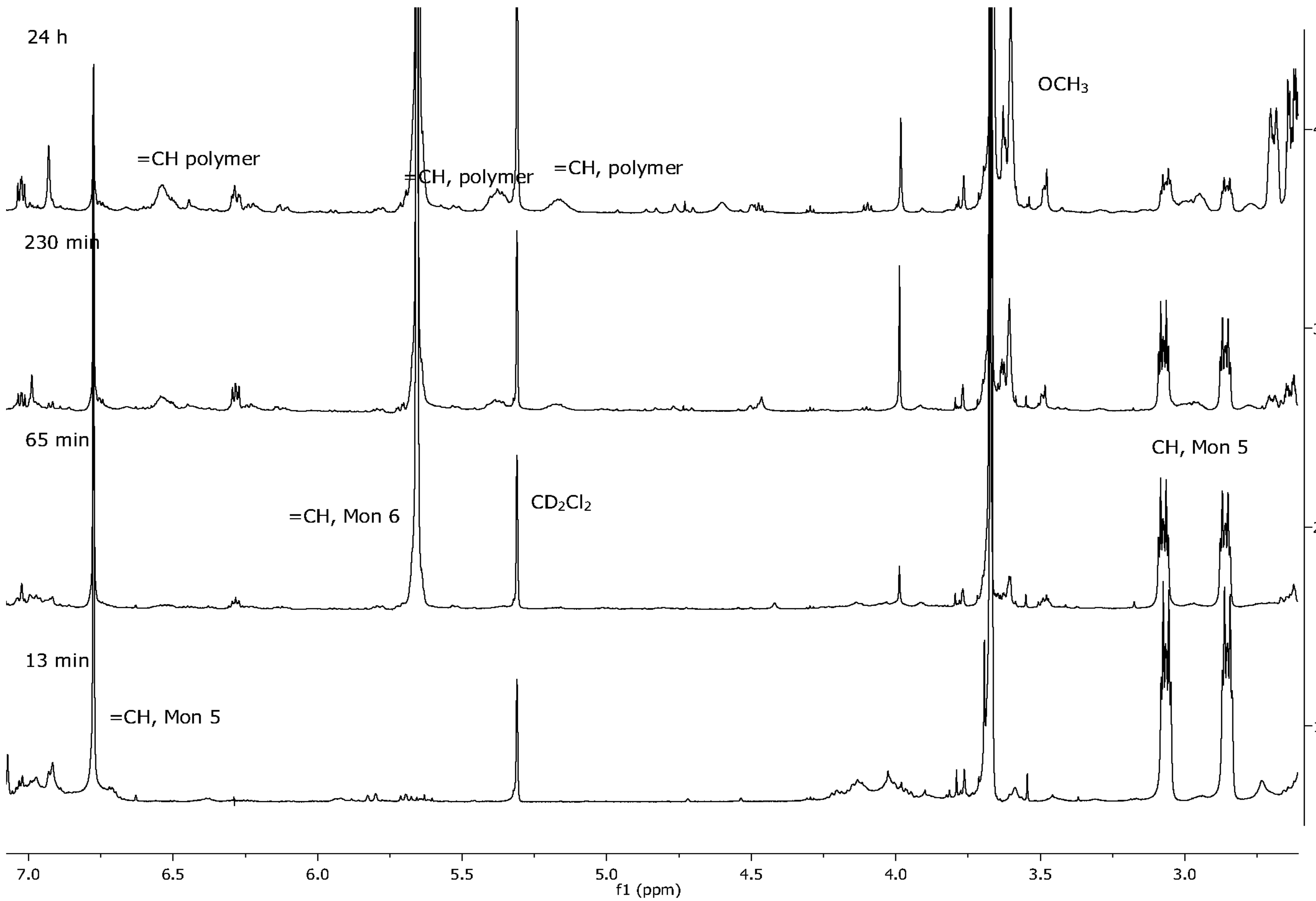

Figure S34. AROMP of monomer **5** and cyclohexene **6** ([**Ru**]:**5**:**6**=1:50:100) in CD_2Cl_2 monitored by ^1H NMR spectroscopy as a function of time.

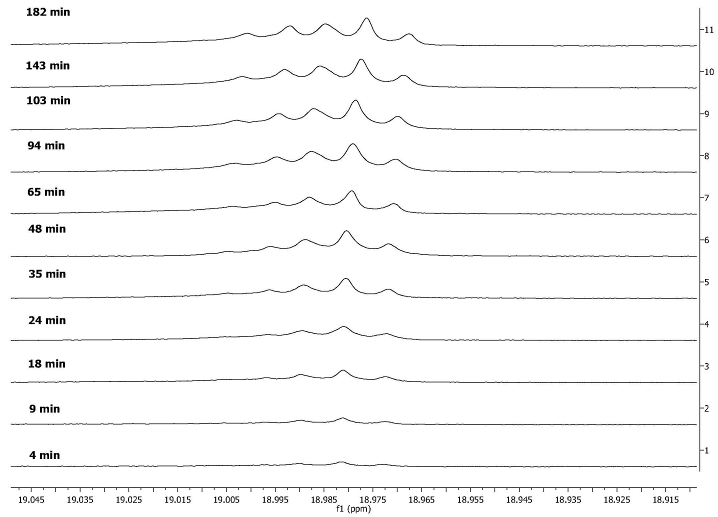

Figure S35. The AROM conversion of [Ru]-**4** enoic carbene to [Ru]-**6**-**4** alkylidene with excess cyclohexene **6** in CD_2Cl_2.

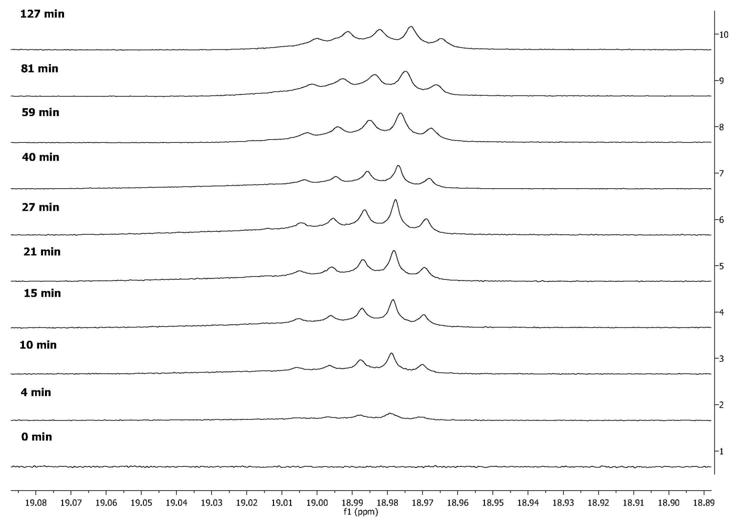

Figure S36. The AROM conversion of [Ru]-**3** enoic carbene to [Ru]-**6**-**3** alkylidene with excess cyclohexene **6** in CD_2Cl_2.

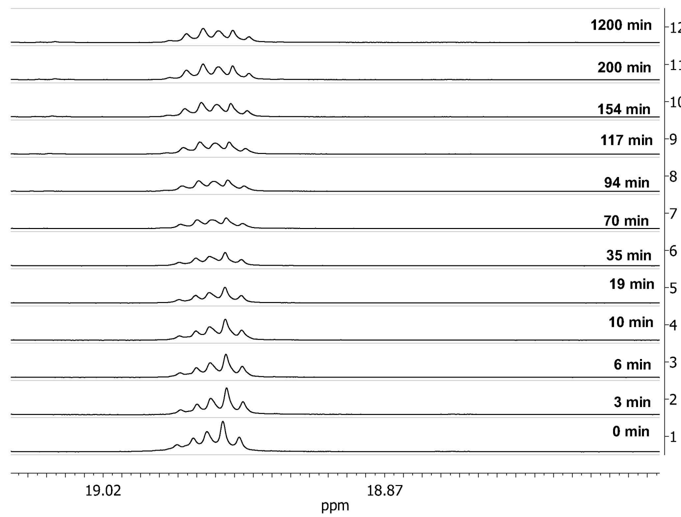

Figure S37. Conversion of [Ru]-**6-4** alkylidene (1 eq) to [Ru]-**6-4-6-4** alkylidene in double AROM (AROM-2) with monomer **4** (1 eq) in the presence of excess cyclohexene **6** in CD_2Cl_2.

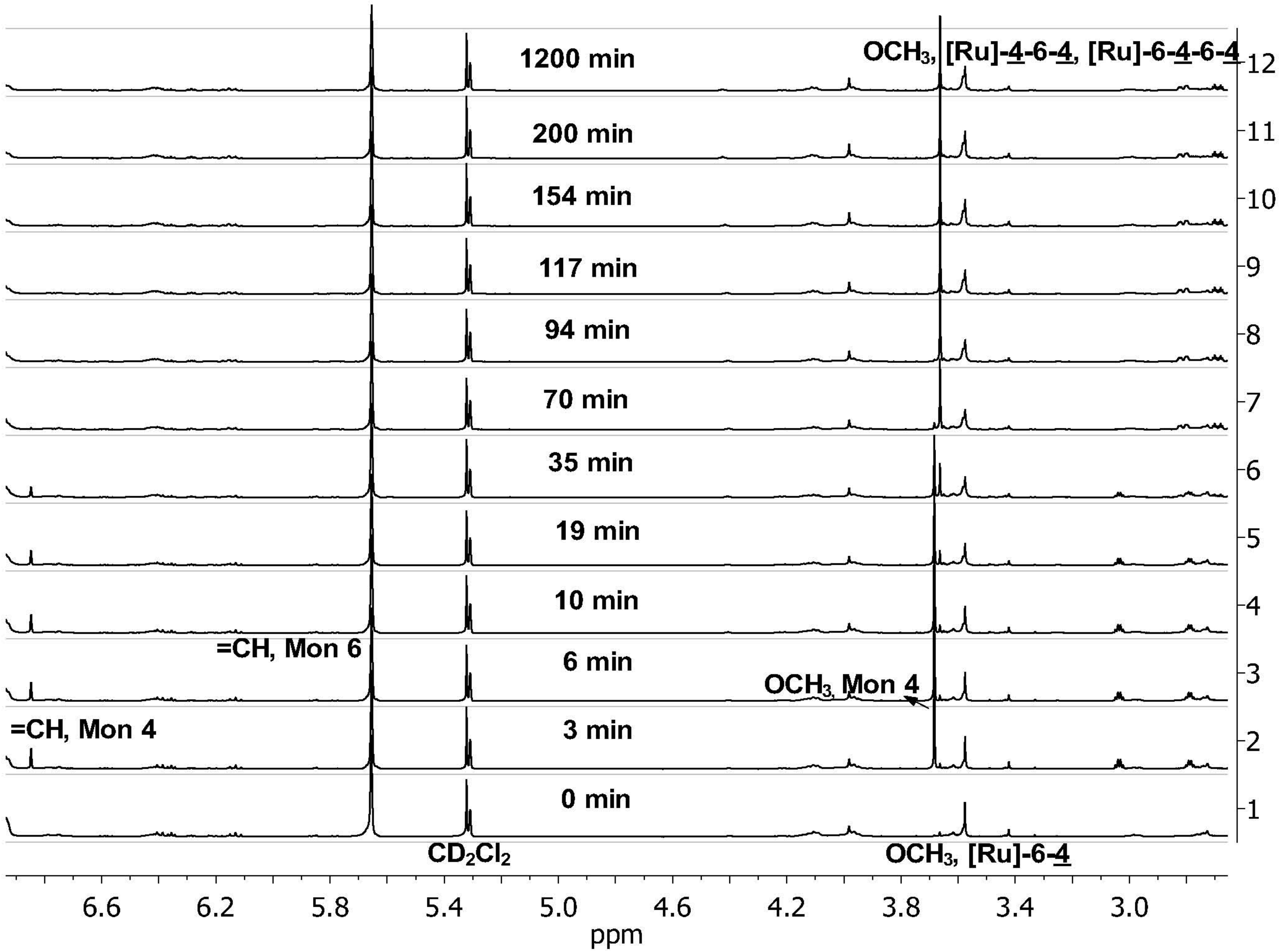

Figure S38. Conversion of monomer **4** (1 eq) in double AROM (AROM-2) with [Ru]-**6**-**4** (1 eq) and excess cyclohexene **6** in CD_2Cl_2.

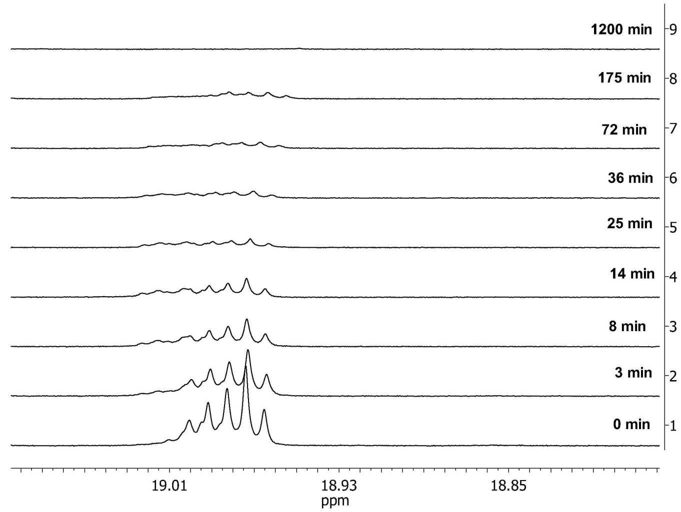

Figure S39. Conversion of [Ru]-**6**-**3** alkylidene (1 eq) to [Ru]-**6**-**3**-**6**-**3** alkylidene in double AROM (AROM-2) with monomer **3** (1eq) in the presence of excess cyclohexene **6** in CD_2Cl_2.

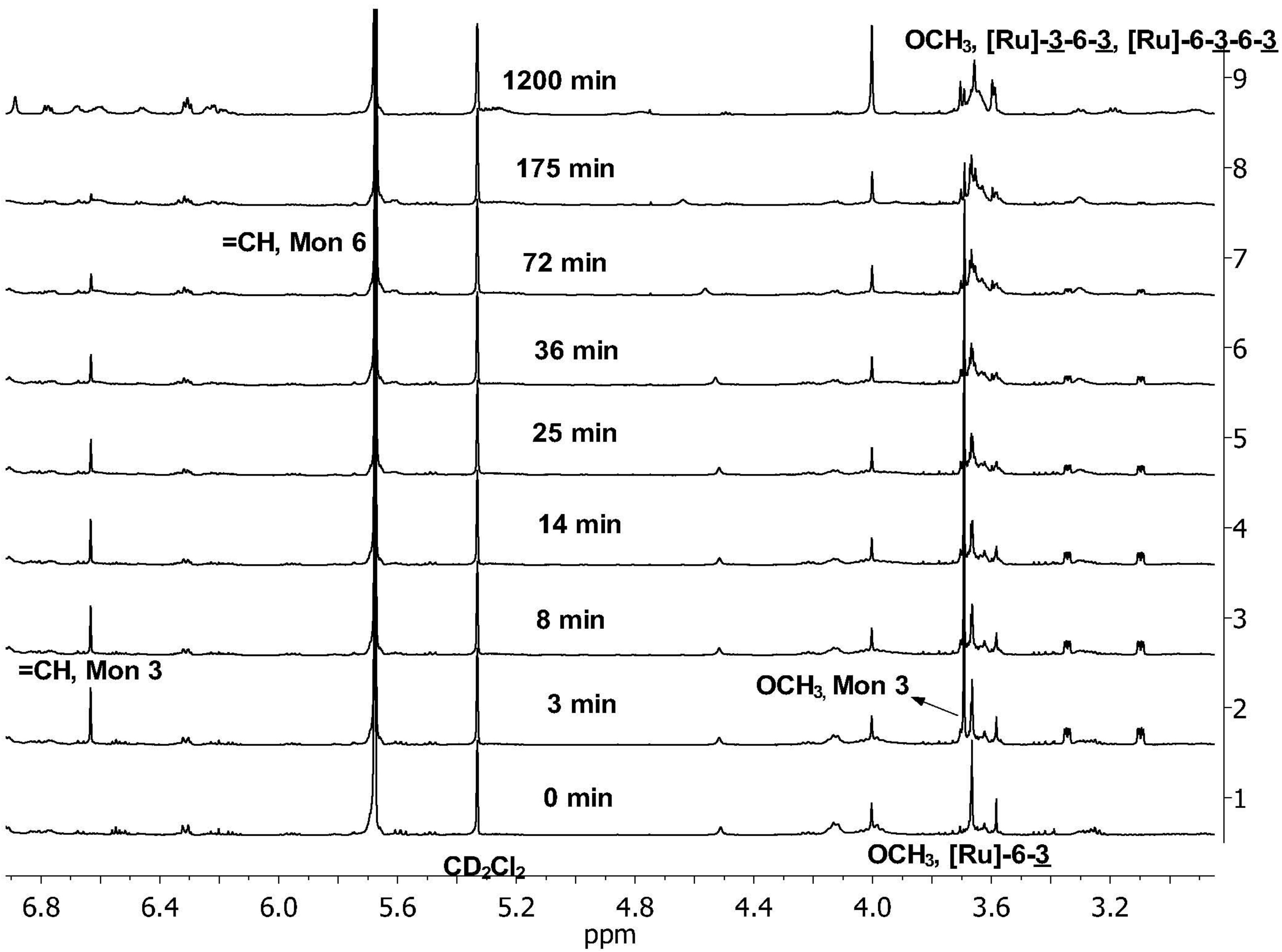

Figure S40. Conversion of monomer **3** (1 eq) in double AROM (AROM-2) with [Ru]-**6**-**3** (1 eq) and excess cyclohexene **6** in CD_2Cl_2.

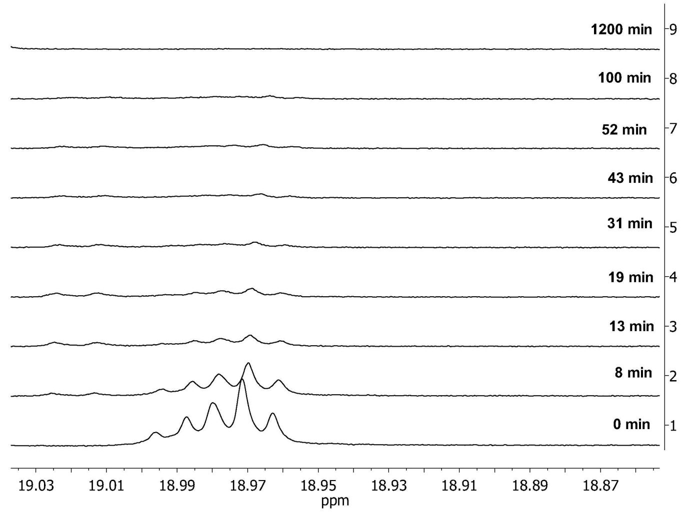

Figure S41. Conversion of [Ru]-**6**-**4** alkylidene (1 eq) to [Ru]-**6**-**3**-**6**-**4** alkylidene in double AROM (AROM-2) with monomer **3** (1 eq) in the presence of excess cyclohexene **6** in CD_2Cl_2.

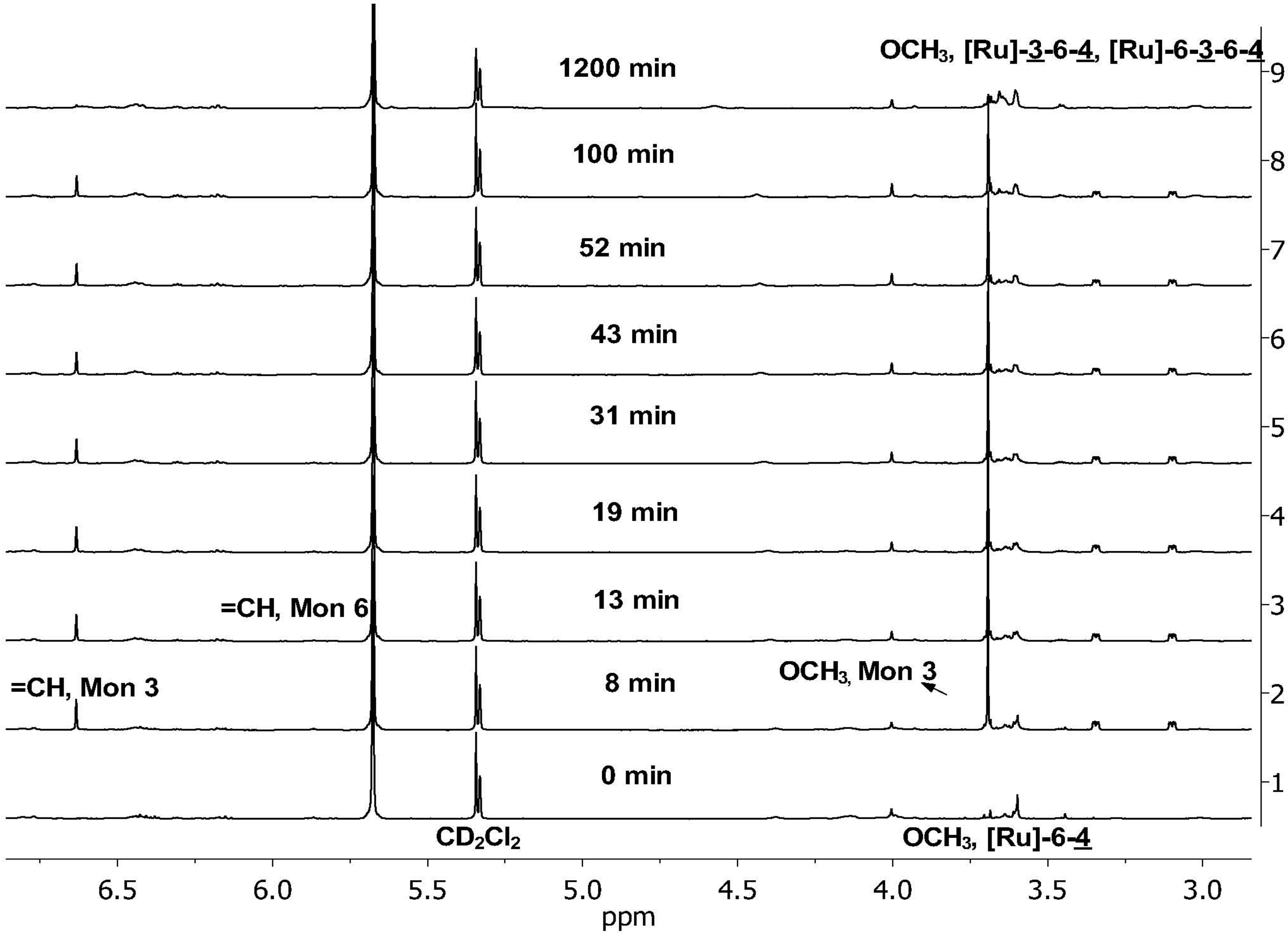

Figure S42. Conversion of monomer **3** (1 eq) in double AROM (AROM-2) with [Ru]-**6**-**4** (1 eq) and excess cyclohexene **6** in CD_2Cl_2.

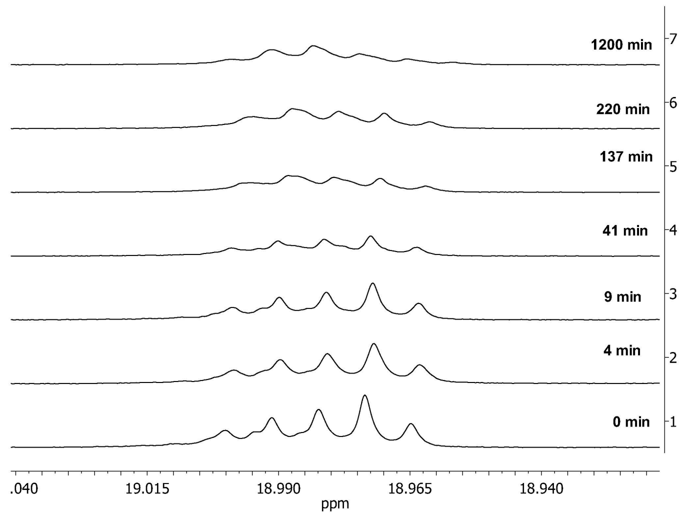

Figure S43. Conversion of [Ru]-**6**-**3** alkylidene (1 eq) to [Ru]-**6**-**4**-**6**-**3** alkylidene in double AROM (AROM-2) with monomer **4** (1 eq) in the presence of excess cyclohexene **6** in CD_2Cl_2.

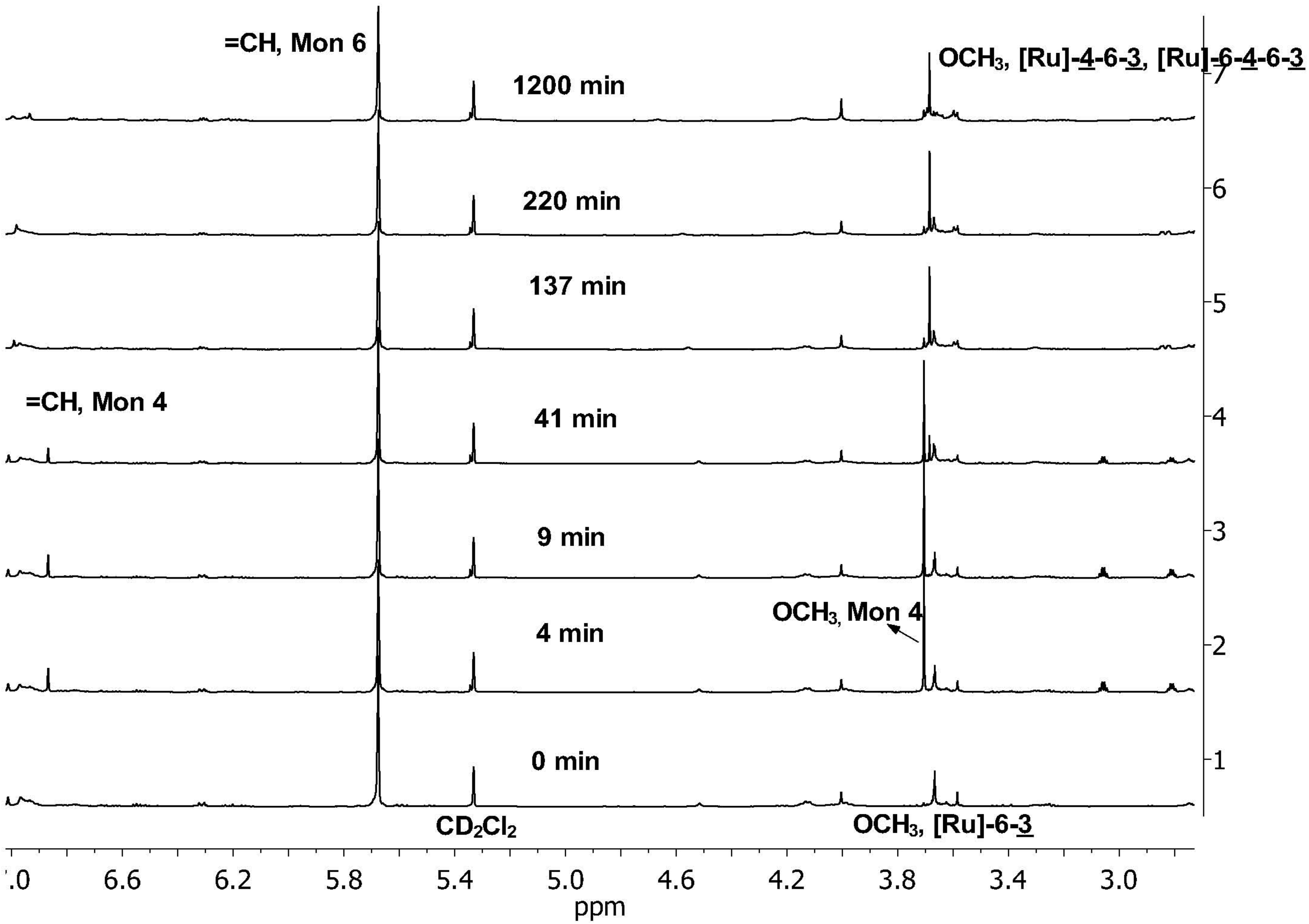

Figure S44. Conversion of monomer **4** (1 eq) in double AROM (AROM-2) with [Ru]-**6**-**3** (1 eq) and excess cyclohexene **6** in CD_2Cl_2.

References

(1) Lapinte, V.; de Frémont, P.; Montembault, V.; Fontaine, L. *Macromol. Chem. Phys.* **2004**, "Ring opening metathesis polymerization (ROMP) of cis- and trans-3,4-bis(acetyloxymethyl)cyclobut-1-enes and synthesis of block copolymers," *205*, 1238-1245. 10.1002/macp.200300224: 10.1002/macp.200300224.